INFLUENCE OF PLASTIC STRAINING ON A YIELD CRITERION

INFLUENCE OF PLASTIC STRAINING ON A YIELD CRITERION

by

MOHAN GURSAHANI, B. Tech. (Hons.)

A Thesis

Submitted to the Faculty of Graduate Studies

in Partial Fulfilment of the Requirements

for the Degree

Master of Engineering

McMaster University

1970

MASTER OF ENGINEERING
(Civil Engineering)

McMASTER UNIVERSITY
Hamilton, Ontario.

TITLE: Influence of Plastic Straining on a Yield Criterion

AUTHOR: Mohan Gursahani, B. Tech. (Hons.)
(Indian Institute of Technology, Bombay)

SUPERVISOR: Dr. R. M. Korol

NUMBER OF PAGES: ix,77

SCOPE AND CONTENTS:

A yield criterion depending on stress, strain and their histories is revised so as to achieve better correlation with experimental data. It is shown that this simple criterion exhibits a reasonable Bauschinger effect. Theoretical expressions for revised yield stresses for two different types of tests are derived for this function.

The purpose of the experimental work in this thesis was to determine the degree of correlation between the proposed function and experimental data. Two types of tests were carried out. The first test was essentially for evaluating the constants appearing in the yield criterion. These values of constants were then used to predict the gross tensile stress-strain curves for specimens cut from sheets which had undergone plastic bending in one direction and contained

residual stresses prior to tensile loading. An approximate method to calculate these residual stresses is also outlined.

Conclusions are deduced by comparing the experimental and theoretical results for these tests and suggestions are made for future research.

ACKNOWLEDGEMENTS

I wish to express my sincere appreciation to Dr. R. M. Korol for his invaluable guidance and encouragement throughout this research programme.

I am thankful to McMaster University for providing sufficient financial support for completion of this thesis.

M. Gursahani

TABLE OF CONTENTS

LIST OF FIGURES

LIST OF PHOTOGRAPHS

LIST OF TABLES

NOMENCLATURE

a	Half thickness of sheet
C	Constant of integration
c	Half width of purely elastic region of sheet
E	Young's modulus of elasticity
F	Scalar function
f	Loading function
J_2	Second stress invariant
K_1, K_2, K_3, K_4	Different values of loading function f
M	Moment required to produce a given bend
M_e	Elastic moment
m, n	Yield criterion constants
R	Radius of bend
S_{ij}	Stress deviator tensor
s, x, y, z	Coordinates
δ_{ij}	Kronecker delta
$\varepsilon_s, \varepsilon_x, \varepsilon_y, \varepsilon_z$	Total strains
$\varepsilon_{s_o}, \varepsilon_{x_o}$	Value of strains when yielding commences
$\varepsilon_x^p, \varepsilon_y^p, \varepsilon_s^p$	Plastic strains
ε_{ij}^p	Plastic strain in tensor notation
$d\varepsilon_{ij}^p$	Plastic increment strain tensor
ν	Poisson's ratio
ν_{av}	Average Poisson's ratio
ν_f	Final Poisson's ratio
$\bar{\sigma}$	Equivalent yield stress

$\sigma_s, \sigma_x, \sigma_y, \sigma_z$	Stresses
$\sigma_{s_o}, \sigma_{x_o}$	Value of stresses when yielding commences
$\sigma_{s_\gamma}, \sigma_{x_\gamma}$	Residual stresses
$\sigma_s^C, \sigma_x^C, \sigma_y^C$	Revised yield stresses in compression
$\sigma_s^T, \sigma_x^T, \sigma_y^T$	Revised yield stresses in tension
σ_s^t, σ_x^t	Stresses required to produce a given total strain
$\sigma_{x(\text{average})}$	Average normal stress
$\sigma_x^{T_e}$	New effective yield stress
$\sigma_y^T(\text{exp.})$	Experimental revised yield stress in tension

CHAPTER 1

INTRODUCTION

All consistent incremental theories of plasticity are closely linked with the concept of a yield criterion which determines whether or not, for a given set of stress increments, further plastic deformation will take place. Loading functions such as octahedral (Von Mises) and maximum shearing stress (Tresca) depending on stresses only are most commonly used. However these criteria, apart from being initially isotropic, are of the isotropic work hardening type. According to these theories, simple tension in any direction affects the material in precisely the same manner as the same amount of tension in any other direction. The yield point is raised equally for all directions and the material when unloaded is truly isotropic [1]. As plastic deformation is physically an anisotropic phenomenon in character, the loading function for a work hardening material must depend on the history of loading and therefore must exhibit *Bauschinger Effect* as well as strain hardening anisotropy even if the material, in the unstrained state, is isotropic. In fact, Drucker [2] has pointed out that an isotropic work hardening theory of plasticity cannot predict a Bauschinger effect during plastic deformation.

1.1 HISTORICAL REVIEW:

Tresca (1864) was the first to suggest a yield criterion for metals. According to his theory metal yielded plastically when the maximum shear stress attained a critical value. Criteria for the yielding of plastic solids, mainly soils, had been proposed and applied before by Coulomb (1773), Poncelet (1848) and Rankine (1853). During the early years of this century various yield criteria were suggested, but for many metals the most satisfactory was that advanced by Von Mises (1913) on the basis of purely mathematical consideration. It was interpreted by Hencky some years afterwards as implying that yielding occurred when the elastic shear-strain energy reached a critical value. Von Mises and Tresca's critera are the most commonly used in practice. However these fail to exhibit a Bauschinger effect. In 1934 Reuss [3] introduced a loading function depending on stress and strain. Theseafter many loading functions which account for various degrees of initial and strain hardening anisotropy as well as a Bauschinger effect have been considered by Drucker [1], Hill [4] and Edelman and Drucker [5]. Edelman and Drucker in their paper "Some extensions of elementary plasticity theory" have examined loading functions of isotropic as well as anisotropic types. These criteria are dealt with in order of increasing complexity and, at the same time, increasing the capacity to represent

experimentally established phenomena.

A yield criterion which includes initial anisotropy has been suggested by Hill [4]. He has considered a state of anisotropy that possesses three mutually orthogonal planes of symmetry at all points but has neglected the Bauschinger effect. It is relevant to mention here that further study in this field has been done by many other authors like Drucker, Svensson and Hillier.

Experimentally it is seen that most of the metals, isotropic at unstrained stage, exhibit Bauschinger effect after plastic straining. Naghdi, Essenburg and Koff [6] in their study of initial and subsequent yield surfaces tested tubular specimens of aluminium alloy. The specimens were subjected to torsion, tension and then reversed torsion. These experiments displayed a pronounced Bauschinger effect although the initial yield surface was almost identical with the Mises yield criterion. The authors suggested that to fit the initial and subsequent yield surfaces of the test, the loading function of an anisotropic strain hardening theory must be employed. However no attempt was made to compare the experimental results with any theory.

Chajes, Britvec and Winter [7] have studied the effect of cold stretching of sheets. They observed that the uniform cold stretching in one direction had a pronounced effect on the mechanical properties of the material, not only

in the direction of stretching but also in the direction normal to it. Regardless of the direction of testing, increase in the yield strength and ultimate strength were found approximately proportional to the prior cold stretching. A comparison of yield strength in tension with that in compression indicated the presence of a Bauschinger effect.

Karren [8,9] studied the effect of various methods of cold forming on the mechanical properties of steel sheets and plates. In his investigation dealing with cold formed corners, flat elements and open sections it was observed that the yield strength after cold forming may be considerably higher than the original ultimate strength of the material. However the increase in yield strength was not the same in all directions, once again indicating the presence of a Bauschinger effect.

1.2 OUTLINE OF RESEARCH

It is evident that an initially isotropic material when subjected to plastic straining exhibits Bauschinger effect and anisotropy. Von Mises and Tresca's criteria are suitable for loading and unloading in only one direction. However for tests involving different loading paths, the predictions made by such criteria are on the unsafe side. Since most of the metals are reasonably isotropic initially, a yield criterion depending on stress, strain and their

histories should be adequate. One such criterion suggested by Edelman and Drucker [5] is revised. It is shown that it exhibits Bauschinger effect with increased capacity and is still relatively simple to use. The purpose of the experimental work in this thesis was to determine the degree of correlation between the proposed function and experimental data. Two types of tests were carried out on two aluminium alloys with different degrees of strain hardening. Three different sheet thicknesses were used to study the limitations of the theory. The theory assumes that material at an unstrained stage is isotropic. It is also assumed that time and temperature effects are small enough to be disregarded. To simulate initial isotropic conditions two perpendicular directions having the same uniaxial stress-strain characteristics were chosen. These directions were determined by carrying out standard tension tests on specimens cut out in various directions.

The next part of the experimental work performed for this thesis consisted of applying tension in the x-direction producing a total strain ε_x, followed by unloading resulting in plastic strain ε_x^p. Next it was loaded in tension in the y-direction. The revised yield stress, σ_y^T, for tension in the y-direction was obtained from the experimental stress-strain curve. The theoretical expressions for the revised yield stresses for tension and compression in both these

directions are derived in terms of two constants. This test was essentially to determine these two arbitrary constants which appear in the suggested yield criterion. Two sets of experimental data are required to evaluate these constants. Once these constants are determined these can then be used to predict the results of any type of loading path. The degree of validity of the proposed theory is then determined in conjunction with another phase to the experimental programme.

The third part of the experimental work consisted of bending sheets about the x-axis to various radii and then allowing elastic springback to occur. Radii before and after springback were measured. Tensile tests were next performed on the curved specimens cut from the bent sheet along the x-axis. The stress-strain curve so obtained is compared with the predicted gross stress-strain curve. An approximate method to predict gross stress-strain curves is outlined in detail.

CHAPTER 2

THEORETICAL ANALYSIS

As described in Chapter 1, two types of tests were performed to see whether reasonable correlation with experimental data could be obtained with the suggested yield criterion which takes plastic strain history into account. Theoretical expressions for revised yield stresses for tension and compression in x and y directions, for these tests, are derived in sections 2.2 and 2.3. Subsequently a method to determine residual stress distribution in a wide metal sheet subjected to cold bending in one direction is outlined in section 2.4.

2.1 Preliminary Discussion:

One of the most common types of yield criteria for ductile materials is known as the Von Mises or maximum energy of distortion type. It is based on homogeneity of behaviour and is therefore independent of coordinate orientation. Yielding for a strain hardening material is governed by the value of a loading function f as it relates to the second invariant of the stresses. Plastic straining occurs if

$$\left.\begin{array}{l} f \geq J_2 \\ \text{while} \quad f < J_2 \end{array}\right\} \qquad (2\text{-}1)$$

describes purely elastic response. The second invariant is described by

$$J_2 = \frac{1}{2} S_{ij} S_{ij} \tag{2-2}$$

where

$$S_{ij} = \sigma_{ij} - \frac{1}{3} \sigma_{kk} \delta_{ij} \tag{2-3}$$

is the stress deviator tensor, as related to the stress tensor σ_{ij}.

For many problems the yield criterion given by (2-1) has been quite satisfactory. The associated flow rule is of the form

$$\left.\begin{aligned} d\varepsilon^p_{ij} &= F \frac{\partial f}{\partial \sigma_{ij}} df \qquad \text{for } df \geq 0 \\ d\varepsilon^p_{ij} &= 0 \qquad\qquad\quad \text{for } df < 0 \end{aligned}\right\} \tag{2-4}$$

where $d\varepsilon^p_{ij}$ is the plastic increment strain tensor while F is a scalar function dependent on the stress state evaluated from a tension test [10]. Equations (2-1) and (2-4) essentially describe isotropic strain hardening and are unreliable for describing non proportional loading problems [11]. When loading along one stress path is followed by complete unloading and then loading in a different stress path predictions are on the unsafe side when using isotropic strain hardening theories. To avoid the complication of a completely general anisotropic yield criterion which relates to the strain history or otherwise [4] the following yield criterion which specializes to Von Mises yielding initially is suggested as

$$f = J_2 - m\,\sigma_{ij}(\varepsilon^p_{ij})^n \qquad (2\text{-}5)$$

where m and n are constants associated with initially isotropic material which characterize behaviour after plastic straining has occurred. The purpose of the remaining sections will be to determine the values of the constants referred to and to relate their evaluation to a practical problem.

2.2 The Effect of Sheet Stretching:

In this test, material is first subjected to tension in the x-direction producing a total strain ε_x. Then it is fully unloaded resulting in a plastic strain ε^p_x and is subsequently subjected to tension in the y-direction. The new yield stress, $\sigma_y{}^T$, for tension in the y-direction is compared with the theoretical value.

For two dimensional problems where σ_x and σ_y are the non trivial principal stresses equation (2-2) simplifies to

$$J_2 = \frac{1}{3}\,(\sigma_x{}^2 - \sigma_x\sigma_y + \sigma_y{}^2). \qquad (2\text{-}6)$$

Furthermore the second term on the right hand side of equation (2-5) can be written as

$$m\sigma_{ij}(\varepsilon^p_{ij})^n = m\sigma_x(\varepsilon^p_x)^n + m\sigma_y(\varepsilon^p_y)^n$$

where m and n are to be determined. For this test the initial stress loading path related to σ_x and σ_y co-ordinates

is OB' (figure 2.1). The flow rule (2-4) associated with the loading function (2-1) for this loading path is

$$\varepsilon_x^p = \varepsilon^p \quad ; \quad \varepsilon_y^p = -\frac{\varepsilon^p}{2}$$

where ε^p is the x-component of plastic strain produced by σ_x^t. The loading function (2-5) at this stage is

$$f = \frac{1}{3}(\sigma_x^2 - \sigma_x\sigma_y + \sigma_y^2) - m\sigma_x(\varepsilon^p)^n - m\sigma_y(\frac{\varepsilon^p}{2})^n = K_2^2 \qquad (2\text{-}7)$$

or

$$\frac{1}{3}[(\sigma_x - \frac{3m(\varepsilon^p)^n}{2})^2 - (\sigma_x - \frac{3m(\varepsilon^p)^n}{2^n})\sigma_y + \sigma_y^2] = K_2^2 + \frac{3}{4}m^2(\varepsilon^p)^{2n} . \qquad (2\text{-}8)$$

For loading path OB'

$$\sigma_x = \sigma_x^t \quad ; \quad \sigma_y = 0$$

hence

$$\frac{1}{3}[\sigma_x^t - \frac{3m(\varepsilon^p)^n}{2}]^2 = K_2^2 + \frac{3}{4}m^2(\varepsilon^p)^{2n} \qquad (2\text{-}9)$$

Now, equation (2-8) can be rewritten as

$$[(\sigma_x - \frac{3m(\varepsilon^p)^n}{2})^2 - (\sigma_x - \frac{3m(\varepsilon^p)^n}{2^n})\sigma_y + \sigma_y^2] = [\sigma_x^t - \frac{3m(\varepsilon^p)^n}{2}]^2 . \qquad (2\text{-}10)$$

The new yield stress for tension and compression in the x-direction is obtained by setting $\sigma_y = 0$ in equation (2-10)

$$\sigma_x^T = \sigma_x^t \qquad (2\text{-}11)$$

$$|\sigma_x^C| = \sigma_x^t - 3m(\varepsilon^p)^n \qquad (2\text{-}12)$$

Similarly, the new yield stresses for tension and compression in the y-direction are obtained by setting $\sigma_x = 0$ in equation

(2-10)

$$\sigma_y^T = + \sqrt{\left[\sigma_x^t - \frac{3m(\varepsilon^p)^n}{2}\right]^2 - \frac{9}{4} m^2 \varepsilon^{2n} + \frac{9m^2\varepsilon^{2n}}{2^{2n+2}}} - \frac{3m(\varepsilon^p)^n}{2^{n+1}} .$$

For small $m(\varepsilon^p)^n$

$$\sigma_y^T \doteq \sigma_x^t - \frac{3m(\varepsilon^p)^n}{2} - \frac{3m(\varepsilon^p)^n}{2^{n+1}}$$

or

$$\sigma_y^T \doteq \sigma_x^t - \frac{3(1+2^n)}{2^{n+1}} m(\varepsilon^p)^n \quad . \tag{2.13}$$

Similarly, the negative radical gives

$$|\sigma_y^C| \doteq \sigma_x^t - \frac{3(2^n-1)}{2^{n+1}} m(\varepsilon^p)^n \tag{2.14}$$

Equation (2.13) forms the basis for evaluating m and n. If for some material two tension tests are conducted with different ε prior to unloading stress σ_x^t then sufficient information becomes available after σ_y^T is obtained.

In figure 2.1, the principal stress plane of σ_x vs. σ_y is shown where the solid curve $f = K_1^2$ represents the initial yield surface, $f = J_2$. The other curves shown with broken lines are plots of $f = K^2 > K_1^2$, for various values of k after the material has been loaded in tension to the point B'.

This simple theory thus allows for the experimentally established fact that a tensile stress beyond initial yield, σ_x^t, produces a yield point in tension which is higher than that in compression in the same direction. For sufficient dilatation of the yield curve, this theory can account for

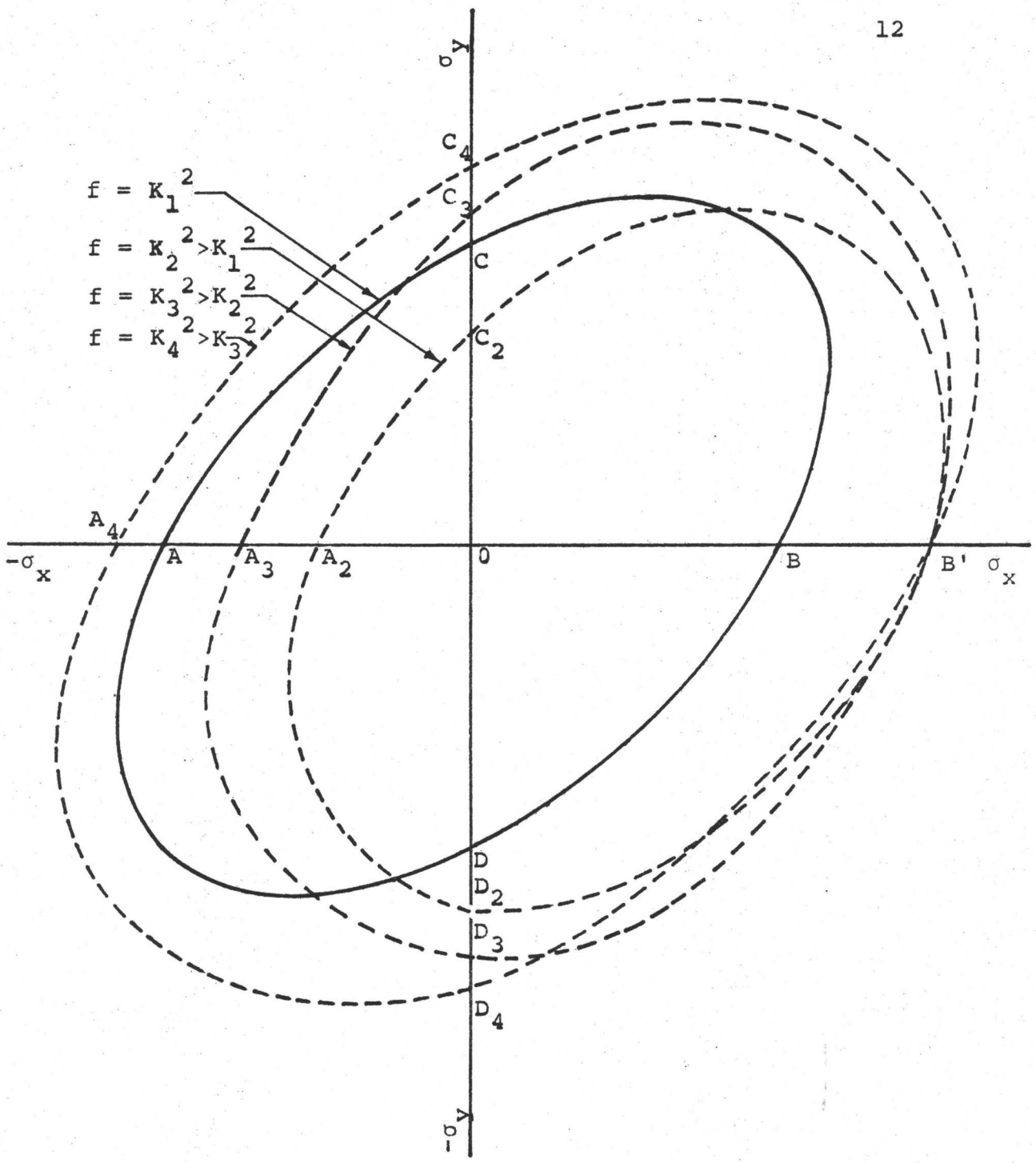

FIG. 2.1 POSSIBLE YIELD CURVES OF $f = J_2 - m\sigma_{ij}(\varepsilon_{ij}^p)^n$ FOR LOADING IN AXIAL TENSION (σ_x) to B'

either hardening such as curve f = K_4, or softening as suggested by curves f = K_2 or K_3, in compression following tension. However in any case OB' is always greater than OA'. For the transverse direction, which experiences a contraction in longitudinal pretension, a higher yield point in subsequent compression than in tension is predicted by this theory. Again, the transverse direction may soften or harden in tension following longitudinal tension. The determination of m and n as described above will uniquely define the correct curve passing through B' in figure 2.1.

2.3 Effect of Sheet Bending:

In this test a wide sheet of metal is first bent about the x-axis to a radius R, producing plastic strains in some of the fibres. Next, it is allowed to springback and subsequently is subjected to tension in the x-direction. The new stress-strain curve for tension in the x-direction is compared with the predicted curve. The theoretical expressions, neglecting residual stresses in the specimen, for σ_x^T, σ_x^C, σ_s^T and σ_s^C are derived as follows. The axes used, for this test, are shown in figure 2.2. Considering σ_s and σ_x only,

$$J_2 = \frac{1}{3} (\sigma_s^2 - \sigma_x\sigma_s + \sigma_x^2) \qquad (2.15)$$

and

$$m\sigma_{ij}(\varepsilon_{ij}^p)^n = m\sigma_s(\varepsilon_s^p)^n + m\sigma_x(\varepsilon_x^p)^n \qquad (2.16)$$

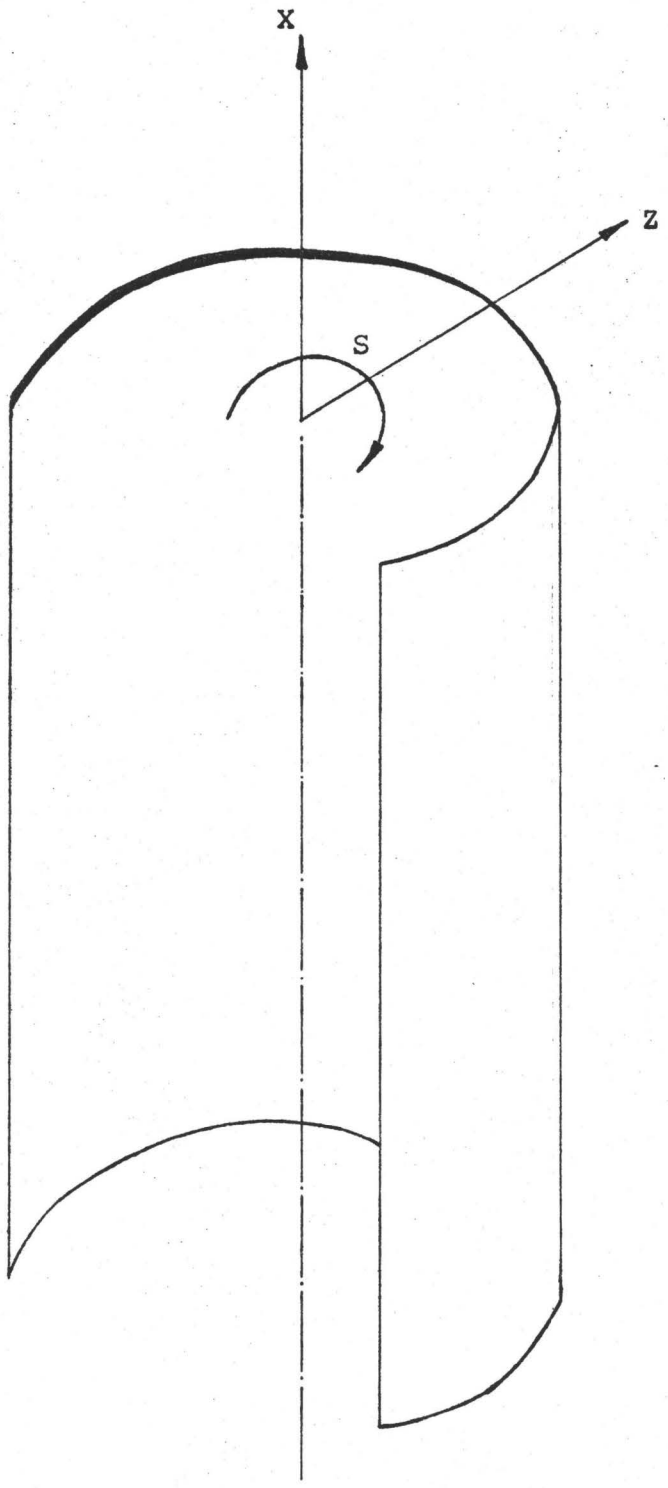

FIG. 2.2 REPRESENTATION OF AXES
FOR COLD BENDING

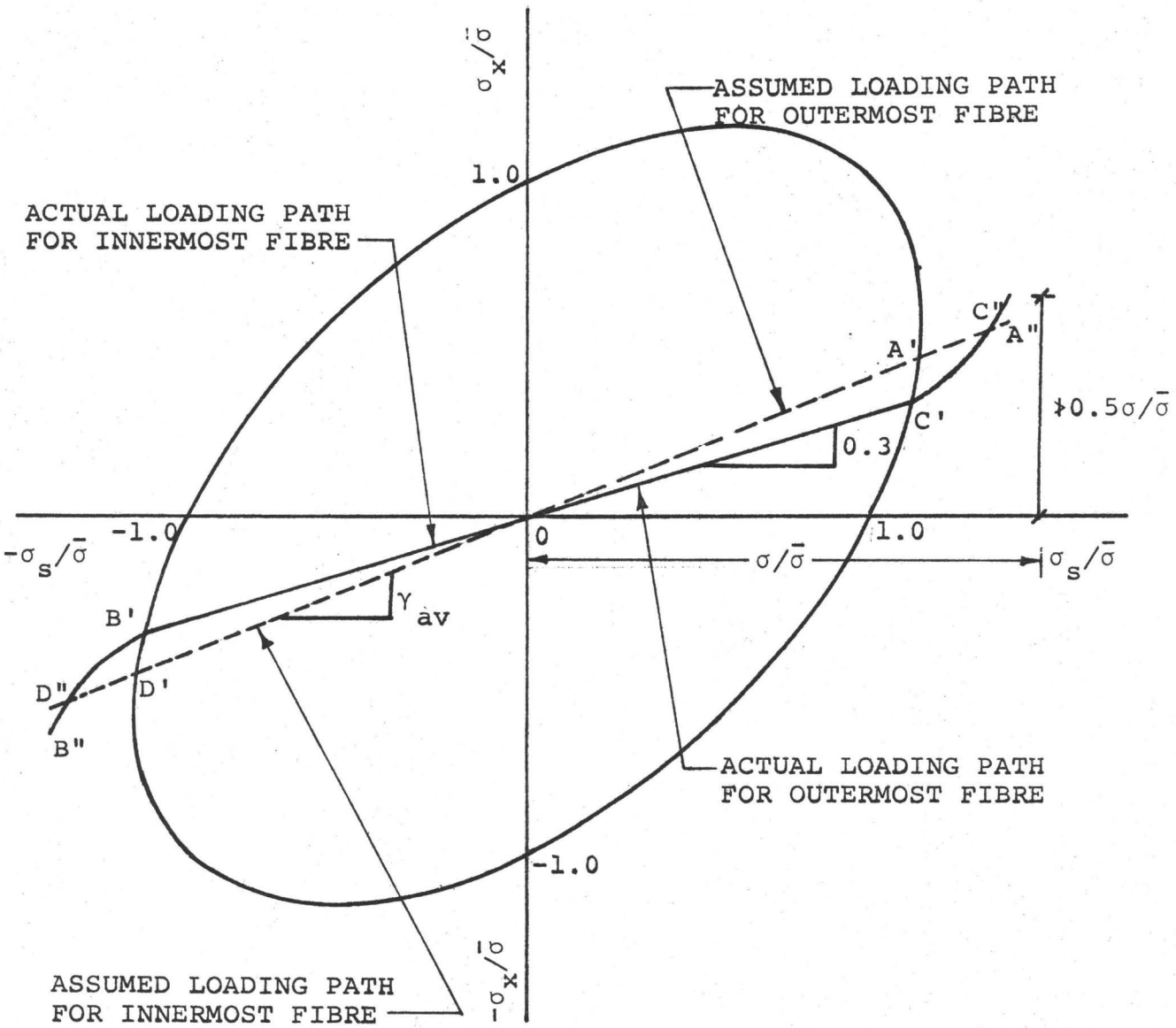

FIG. 2.3 LOADING PATHS IN BENDING

In this test, the actual loading path for the outermost fibre is OC'C" (fig. 2.3). As the plastic strain increases, the Poisson's ratio increases and in the limit reaches its maximum value of 0.5. However, for simplicity Poisson's ratio is assumed to be constant. An average value of Poisson's ratio is taken which is calculated for each element by

$$\nu_{av} = (\nu_f - 0.3)\frac{\varepsilon^p}{\varepsilon} + 0.3 \qquad (2.17)$$

where ν_f is Poisson's ratio, defined by σ_x/σ_s, at total strain ε to which the element in question is subjected. Hence the assumed loading path for the outermost fibre is OA'A" as shown in figure 2.3. Similarly, OB'B" and OD'D" are actual and assumed loading paths for the innermost fibres. For the assumed loading path OA'A"

$$\varepsilon_s^p = \varepsilon^p \quad ; \quad \varepsilon_x^p = 0.$$

The loading function, $f = J_2 - m\sigma_{ij}(\varepsilon_{ij}^p)^n$, at this stage is

$$f = \frac{1}{3}(\sigma_s^2 - \sigma_s\sigma_x + \sigma_x^2) - m\sigma_s(\varepsilon^p)^n = K_2^2 \qquad (2\text{-}18)$$

or,

$$f = \frac{1}{3}[(\sigma_s - \frac{3}{2}\, m(\varepsilon^p)^n)^2 - \sigma_s\sigma_x + \sigma_x^2] = k_2^2 + \frac{3}{4}\, m^2(\varepsilon^p)^{2n} \qquad (2.19)$$

For loading path OA'A"

$$\sigma_s = \sigma_s^t \quad ; \quad \sigma_x = \nu_{av.}\, \sigma_s^t$$

hence,

$$\frac{1}{3}[(\sigma_s^t - \frac{3}{2}\, m(\varepsilon^p)^n)^2 - \nu_{av.}\, \sigma_s^{t2} + \nu_{av.}^2 \sigma_s^{t2}] = k_2^2 + \frac{3}{4}\, m^2(\varepsilon^p)^{2n} \qquad (2.20)$$

Now equation (2-19) can be rewritten as,

$$[(\sigma_s - \tfrac{3}{2} m(\varepsilon^p)^n)^2 - \sigma_s\sigma_x+\sigma_x^2] = [(\sigma_s^t - \tfrac{3}{2} m(\varepsilon^p)^n)^2-\nu_{av}\sigma_s^{t^2} + \nu_{av}^2\sigma_s^{t^2}] \quad (2.21)$$

The new yield stress for tension and compression in the s-direction is obtained by setting $\sigma_x = 0$ in equation (2.21)

$$\sigma_s^T = \sqrt{[(\sigma_s^t - \tfrac{3}{2} m(\varepsilon^p)^n)^2 - \nu_{av}\sigma_s^{t^2} + \nu_{av}^2 \sigma_s^{t^2}]} + \tfrac{3}{2} m(\varepsilon^p)^n \quad (2.22)$$

$$|\sigma_s^C| = \sqrt{[(\sigma_s^t - \tfrac{3}{2} m(\varepsilon^p)^n)^2 -\nu_{av}\sigma_s^{t^2} + \nu_{av}^2\sigma_s^{t^2}]} - \tfrac{3}{2} m(\varepsilon^p)^n \quad (2.23)$$

The new yield stress for tension and comparison in the x-direction is obtained by setting $\sigma_s = 0$ in equation (2.21)

$$\sigma_x^T = |\sigma_x^C| = \sqrt{[\sigma_s^{t^2}(1-\nu_{av}+\nu_{av}^2) - 3m\sigma_s^t(\varepsilon^p)^n]} \quad (2.24)$$

The fibres undergoing compression while bending follow loading path OD'D". The above expressions, (2.22), (2.23) and (2.24), are valid except for the fact that expressions for σ_s^T and σ_s^C are interchanged.

2.4 Residual Stress Analysis:

The analysis outlined in this section shows a method for predicting the residual stress distribution in a wide metal sheet which is first subjected to cold bending in one direction and then is allowed to springback. Initially, stresses and strains in the sheet prior to springback are obtained, to a good approximation, using the classical elastic

and plastic theories. Subsequently, a method is outlined which enables the residual stress distribution, in both longitudinal and circumferential directions, to be obtained.

2.4.1 Elastic Stress-Strain Relations:

The initial bending of the metal sheet is purely elastic and if at this stage the force is removed, the sheet will springback to its flat position. Further bending causes the outer fibres of the sheet to yield and hence a permanent strain will result. As shown in figures 2.4(a) and 2.4(b), the condition arises where the centre core of the cross-section is elastic, defined by parameter 2c in figure 2.4(a), and the outer fibres are plastic. As bending is continued, the thickness of this elastic core decreases and hence the ratio of thickness to elastic core, a/c, increases.

It is assumed in this analysis that the width of the sheet is much greater than the thickness, thus the anti-elastic curvature is concentrated at the ends [12]. It is also assumed that the transverse planes remain plane in bending. From these conditions it can be assumed that

$$\sigma_z = 0 \quad ; \quad \varepsilon_x = 0 \qquad (2.25)$$

At the initial yield point, for any fibre, the suggested yield criterion is equivalent to Von Mises criterion. Hence,

$$f = J_2$$

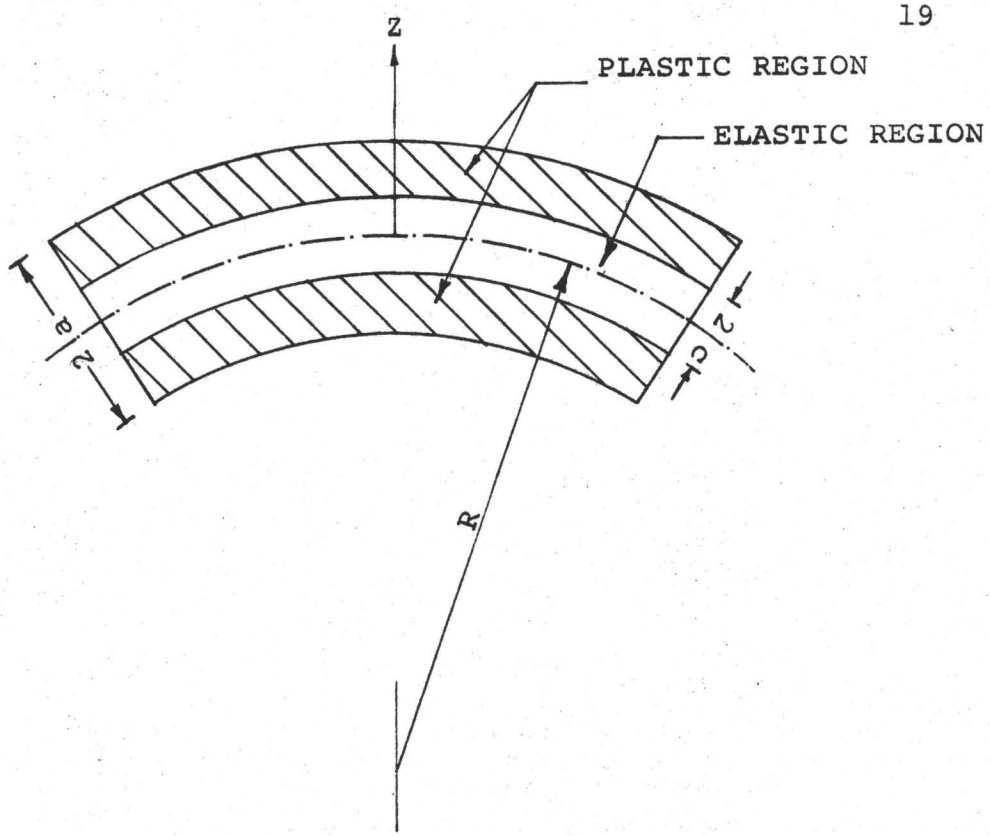

FIG. 2.4(a) METAL SHEET DURING BENDING

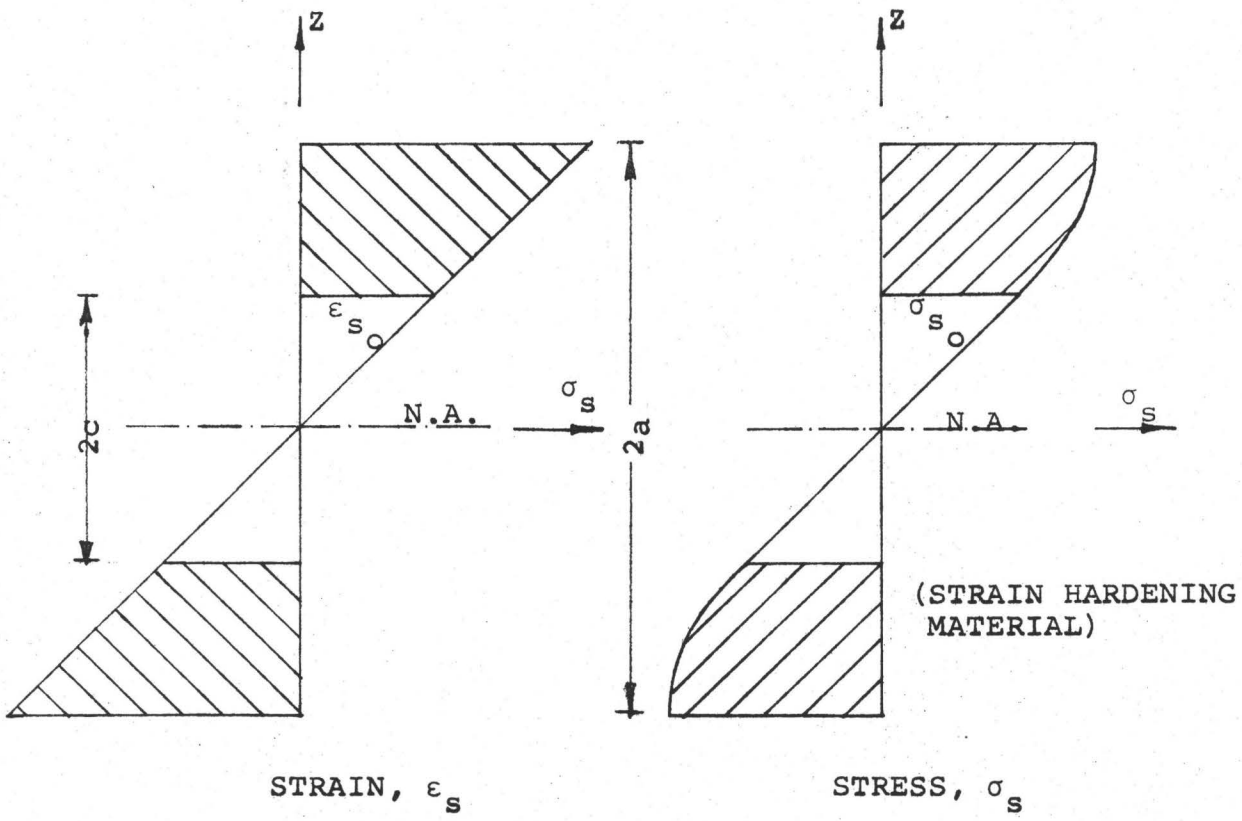

FIG. 2.4(b) STRESSES AND STRAINS THROUGH CROSS-SECTION

or

$$\sigma_s^2 - \sigma_s\sigma_x + \sigma_x^2 = \bar{\sigma}^2 \tag{2.26}$$

where $\bar{\sigma}$ is the equivalent initial yield stress.

By using the elastic condition

$$\sigma_x = \nu\sigma_s \tag{2.27}$$

the circumferential stress at commencement of yield,

$$\sigma_{s_o} = \frac{\bar{\sigma}}{\sqrt{(1-\nu+\nu^2)}} \tag{2.28}$$

Circumferential strain at the instant of yielding

$$\varepsilon_{s_o} = \frac{\sigma_{s_o}}{E}(1-\nu^2) = \frac{1-\nu^2}{\sqrt{(1-\nu+\nu^2)}}\frac{\bar{\sigma}}{E} \tag{2.29}$$

Assuming a value of 0.3 for Poisson's ratio,

$$\left.\begin{aligned} \sigma_{s_o} &= 1.127\ \bar{\sigma} \\ \varepsilon_{s_o} &= 1.025\ \bar{\sigma}/E \\ \sigma_{x_o} &= 0.338\ \bar{\sigma} \end{aligned}\right\} \tag{2.30}$$

2.4.2 Incremental Stress-Strain Analysis:

To obtain a theoretical prediction of the complete stress-strain curve for the bending of a sheet, the strain hardening portion of the curve must be analysed. For an ideal elastic plastic material, Alexander [13] has obtained the solution, which is given here in the form used by Daniels [14].

$$E(\varepsilon_s - \varepsilon_{s_o}) = (1-2\nu)\sigma_x - \frac{\bar{\sigma}\sqrt{3}}{4}\log\left|\frac{\frac{2}{\sqrt{3}}\bar{\sigma} - \sigma_s}{\frac{2}{\sqrt{3}}\bar{\sigma} + \sigma_s}\right| + C \tag{2.31}$$

where

$$C = \frac{\sqrt{3}}{4}\bar{\sigma}\log\left|\frac{2\sqrt{(1-\nu+\nu^2)} - \sqrt{3}}{2\sqrt{(1-\nu+\nu^2)} + \sqrt{3}}\right| - \frac{\nu\bar{\sigma}(1-2\nu)}{\sqrt{(1-\nu+\nu^2)}} \qquad (2.32)$$

This solution is obtained on the assumption that the material follows Von Mises yield criterion. A good approximate solution for a strain hardening material can be obtained using the above solution. For an ideally elastic-plastic material the loading path follows the yield curve and hence equation (2.26) is satisfied for all values of strain as $\bar{\sigma}$ is constant. In other words, the yield curve neither translates nor dilatates. However, in the case of a strain hardening material $\bar{\sigma}$ increases as the strain increases. To account for Bauschinger effect it is necessary that the yield curve should translate as well as dilatate with the increase of plastic strain. If Bauschinger effect is neglected the yield curve should only dilatate. To predict an approximate stress-strain curve it is assumed that there is no Bauschinger effect. It is also assumed that $\bar{\sigma}$ remains constant over a small increment of strain.

On the basis of these assumptions the principal stress-strain curves are computed as follows. First, for a value of $\sigma_x = 0.34\ \bar{\sigma}$ (eqn. 2.30), σ_s and ε_s are computed using equations (2.26), (2.31) and (2.32). For this value of ε_s the corresponding value of equivalent strain ε which for uniaxial tension or compression becomes actual strain, is calculated

using the new value of Poisson's ratio in equation (2.29), rewritten as

$$\varepsilon = \frac{\bar{\sigma}}{E} = \frac{\sqrt{(1-\nu+\nu^2)}}{(1-\nu^2)} \varepsilon_s \qquad (2.29)$$

The stress, σ , corresponding to the value of ε obtained above is calculated using the stress-strain characteristic of the material as obtained by a standard tension test. $\bar{\sigma}$ can be shown to be equivalent to σ so obtained by invoking equation (2.26). This value of $\bar{\sigma}$ is used in the equations (2.26), (2.31) and (2.32) as σ_s and ε_s are computed for the next higher value of σ_x and the cycle is repeated. For computation purposes, the stress-strain curve for the material is divided into a number of parts in such a way that the stress-strain relation is piece-wise linear. These computations are done using the CDC6400 available at McMaster University. The computer program used is given in Appendix 1. The values of σ_s, ε_s and σ_x so obtained are plotted as shown in fig. 2.5. These curves describe the stress-strain characteristics in two directions of an element in the cross-section of a thin sheet which is subjected to bending into the plastic range.

2.4.3 Residual Stresses on Springback:

The curves in figure 2.5 can also show the complete stress distribution throughout the whole cross-section of the

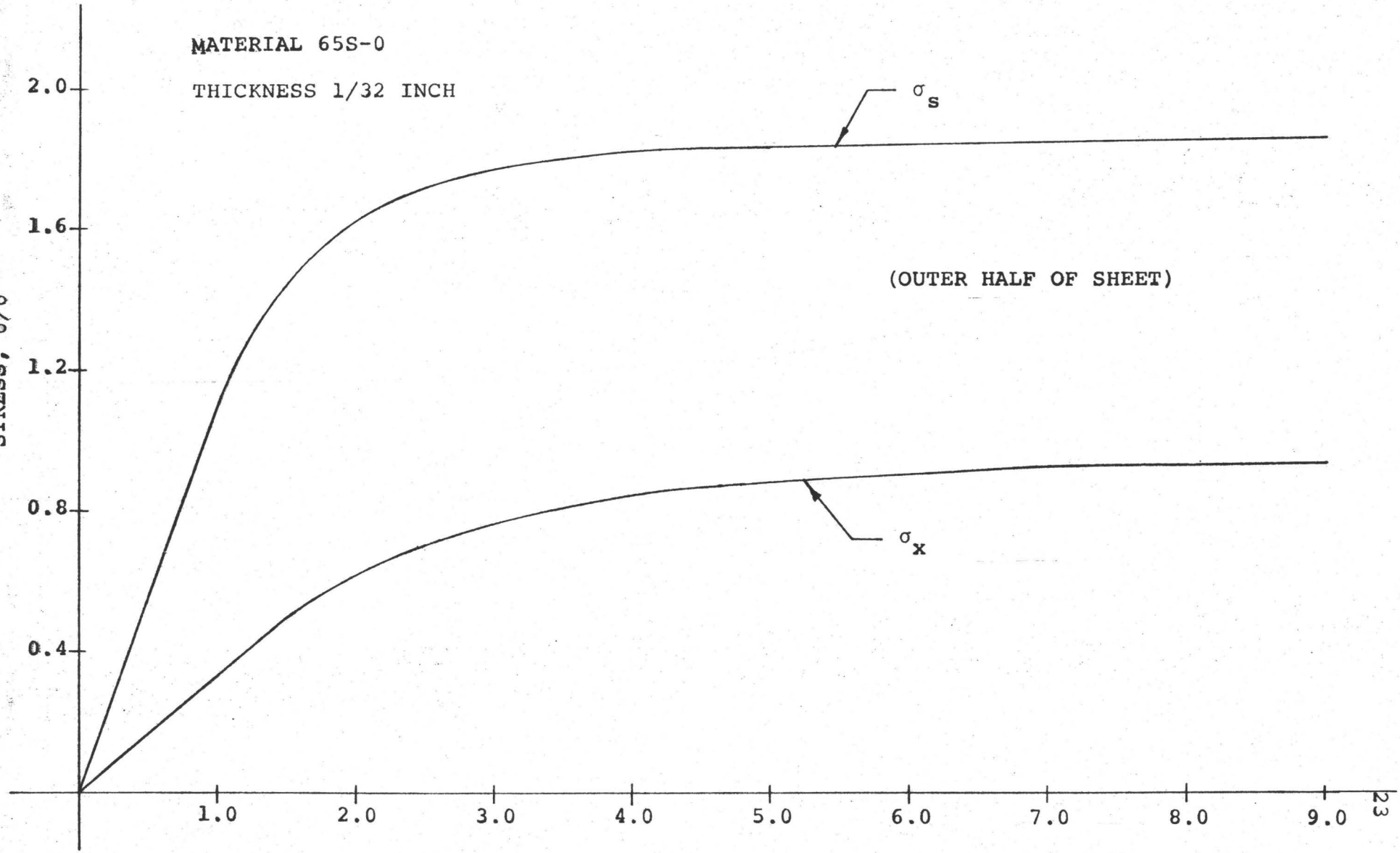

FIG. 2.5 THEORETICAL STRESS-STRAIN CURVE FOR BENDING

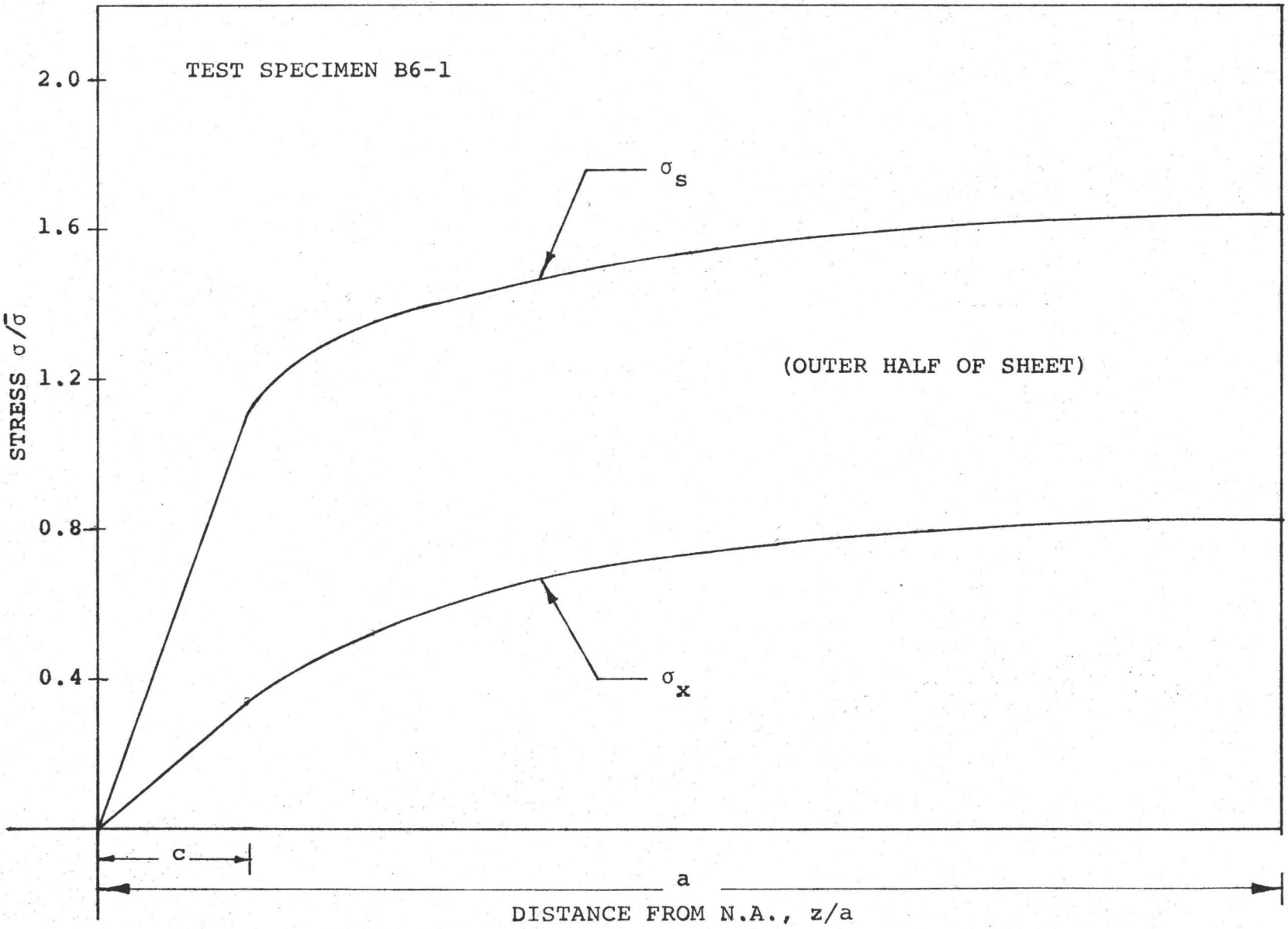

FIG. 2.6 STRESS DISTRIBUTION PRIOR TO SPRINGBACK

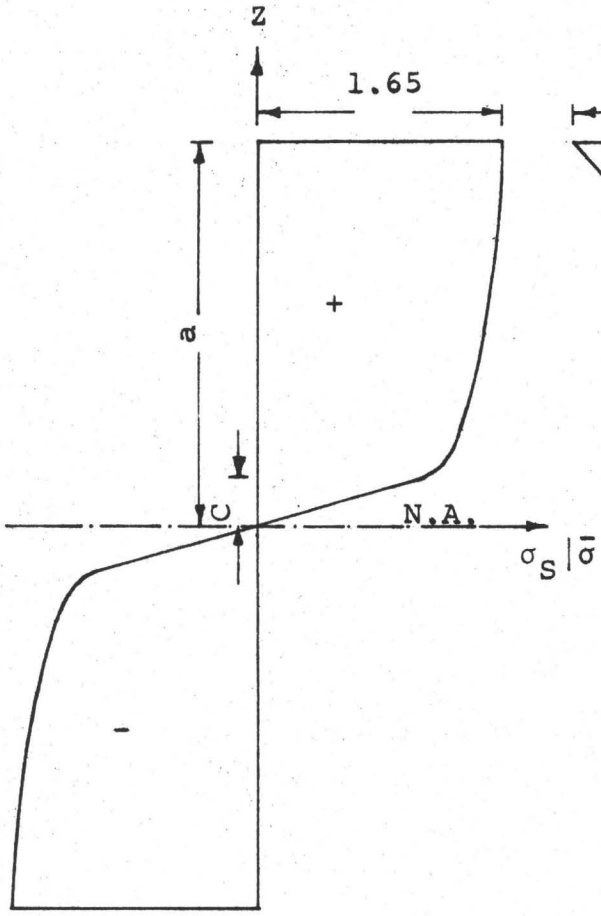

FIG. 2.7(a)

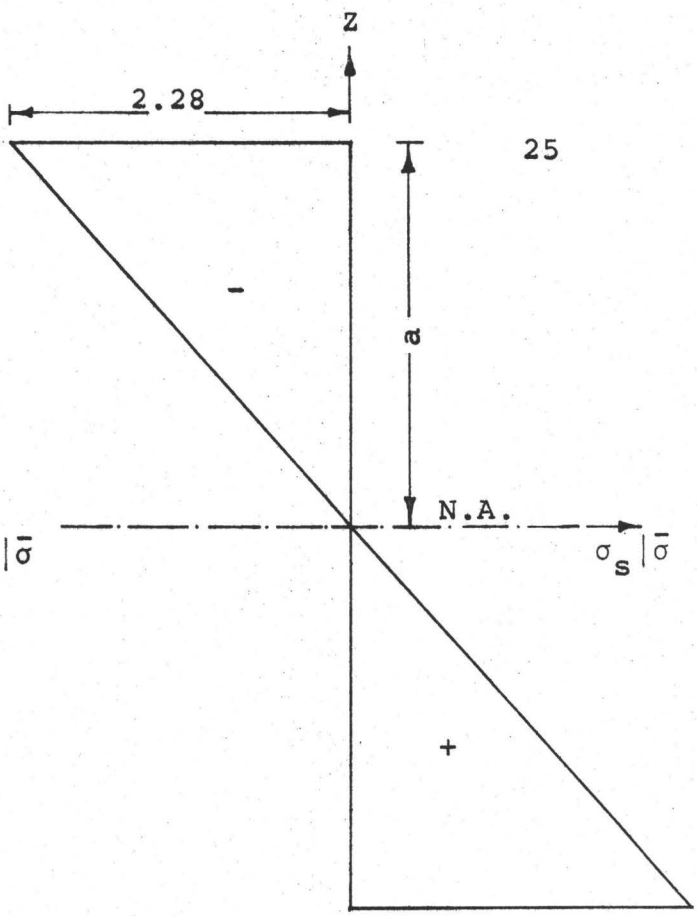

FIG. 2.7(b)

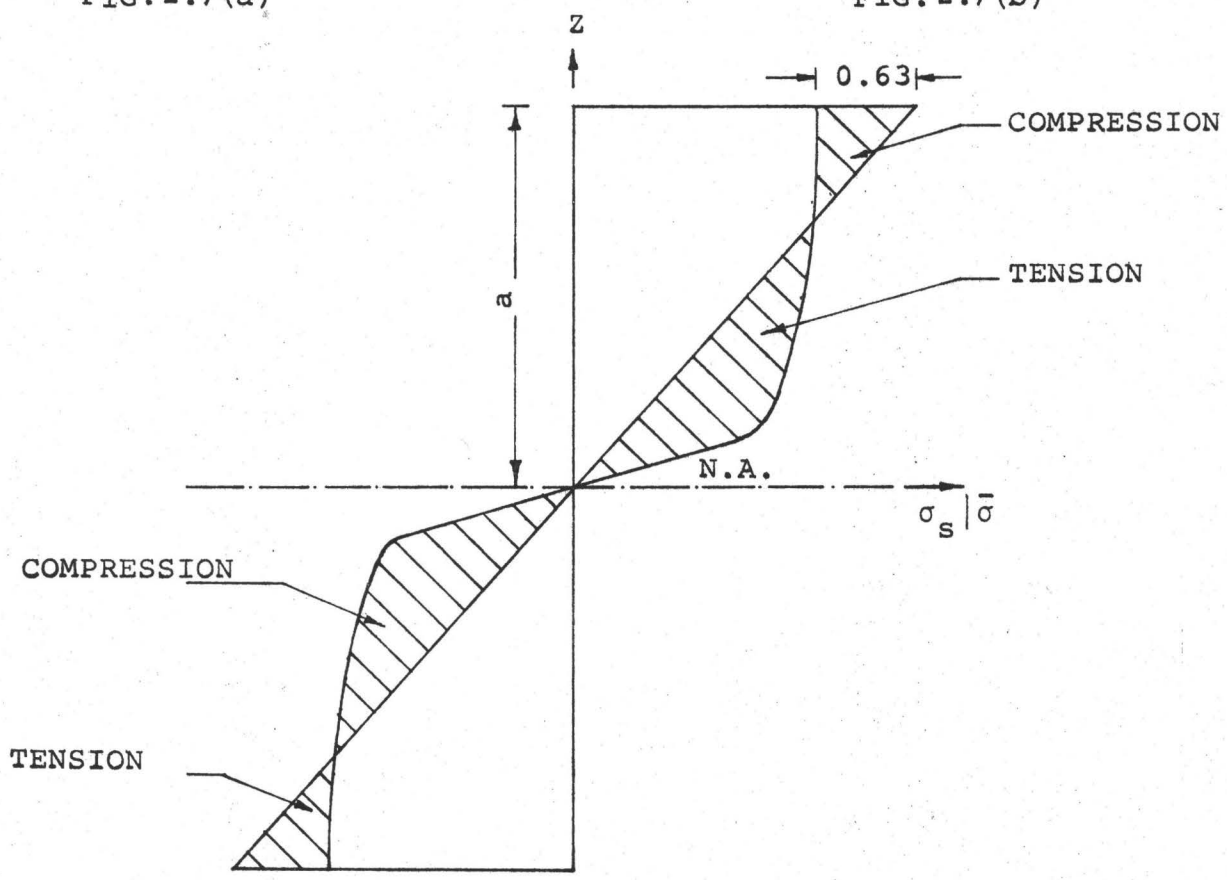

FIG. 2.7(c) RESIDUAL STRESS DISTRIBUTION IN CIRCUMFERENTIAL DIRECTION

sheet for a particular radius of bend. This is done by drawing the curves in such a way that the ratio of the elastic portion of the curve to the complete curve is the same as a particular value of the ratio, c/a. For one of the specimens this is shown in figure 2.6. When this is achieved, the stress distribution before springback is obtained and the strain axis also becomes equivalent to a measure of the distance of the various fibres from the neutral axis of the sheet. Figure 2.7(a) shows the complete stress distribution, for one of the specimens, prior to springback. This enables one to calculate the moment, M, required to produce a given radius of bend. When the sheet is allowed to springback, unloading is purely elastic and hence the superimposed stress distribution during unloading will be linear across the section, figure 2.7(b). The complete stress distribution can be obtained using the moment equilibrium condition about the x-axis. The elastic moment, M_e, should be equal but opposite in sign to M. By superimposing the elastic stress distribution on the stress distribution prior to springback gives the resultant residual stress (σ_{s_γ}) distribution in the circumferential direction as shown in figure 2.7(c).

Next, to predict the residual stress distribution in the longitudinal direction a graphical construction is employed. The sheet thickness is divided into nine discrete elements, figure 2.8. In bending each of these elements

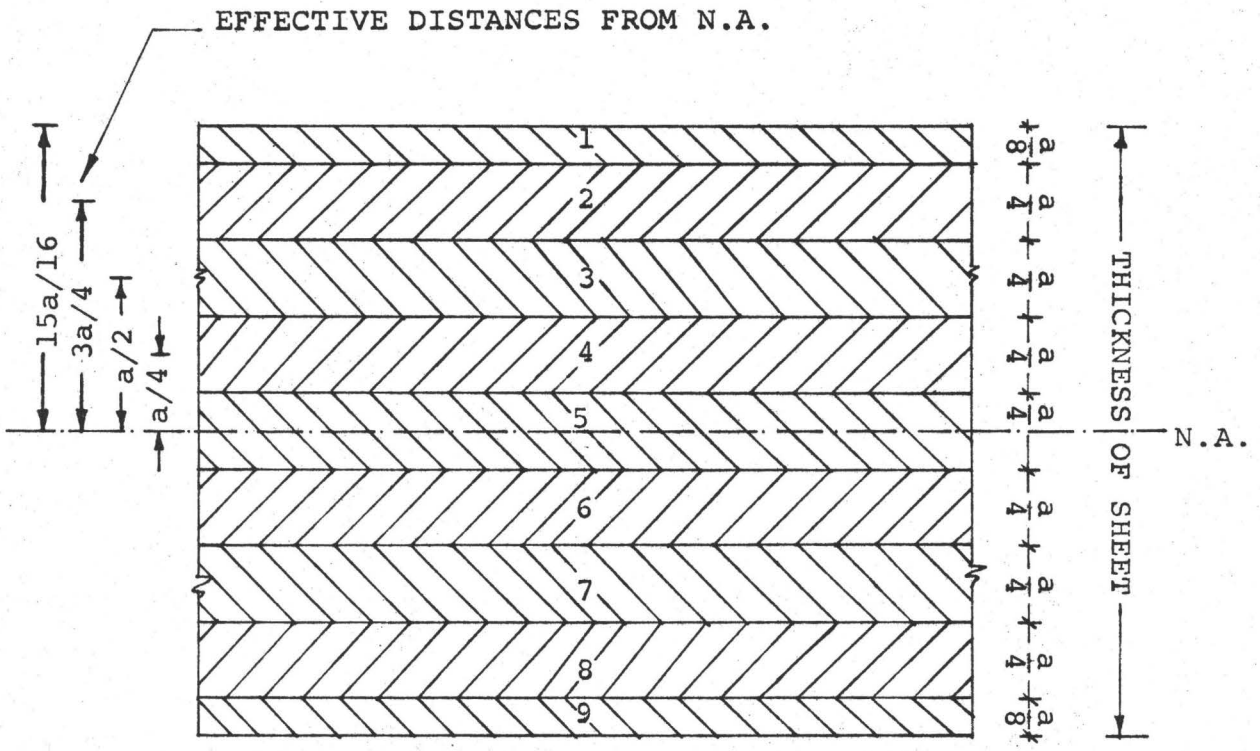

FIG. 2.8 ARRANGEMENT OF ELEMENTS

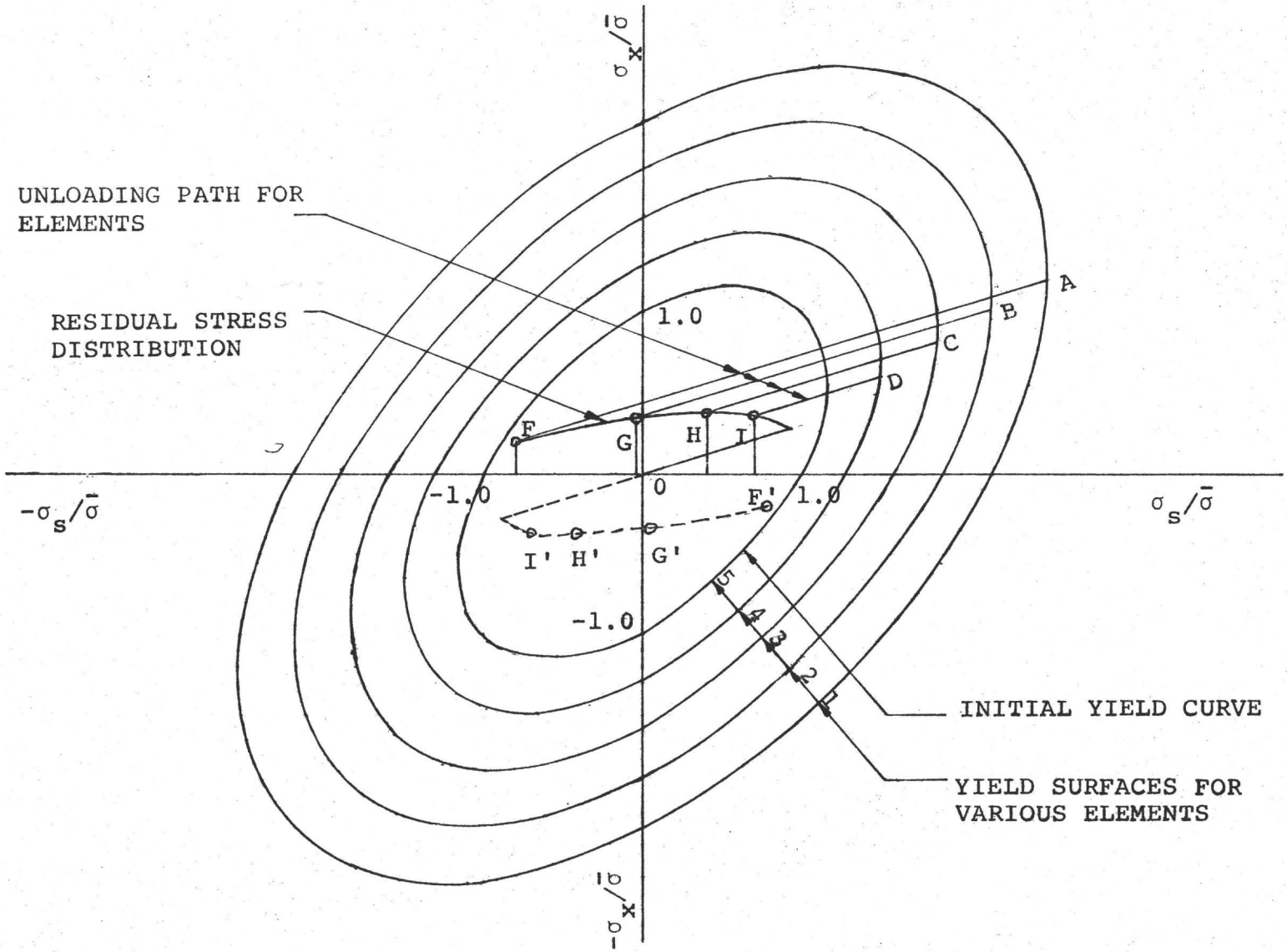

FIG. 2.9 RESIDUAL STRESS DISTRIBUTION

undergoes a different plastic strain and hence each has a different loading path. The new yield curve for each of these elements will also be different. It is assumed that constants m and n determined in section 2.2 apply to all the elements in the sheet. For simplicity, Bauschinger effect at this stage is neglected and hence the yield curves will be co-centric ellipses as shown in figure 2.9. Points A,B,C,D and O represent stress state prior to springback of elements 1,2,3,4 and 5 respectively. As unloading is purely elastic, ν=0.3, the unloading path for each of these elements will be as shown in figure 2.9. The residual stress in the circumferential direction, σ_{s_γ} for each element can be obtained from figure 2.7(c). The intersection of the unloading path with the corresponding ordinate representing σ_{s_γ} for the element gives the residual stress in longitudinal direction, σ_{x_γ}. Thus in figure 2.9, points F,G,H,I and O represent the residual stress state for elements 1,2,3,4 and 5 respectively. Curve FGHIO gives the residual stress distribution for the outer half thickness of the sheet. For the inner half thickness, it will be similar but opposite in sign as given with broken line F'G'H'I'O.

Having thus obtained this residual stress distribution, it is necessary to consider its effect on the longitudinal stress-strain characteristics in tension. As each element

with a different relative position with respect to the neutral axis was subjected to a different loading condition, each possesses a different strain history in bending. Thus, following cold bending each element has a different state of residual stress and is associated with its own yield surface. The new yield surface should take Bauschinger effect into account otherwise the theoretical predictions will be on the unsafe side. The method to predict the new stress-strain curve for tension in the x-direction following bending about x-axis is outlined, in detail, in chapter 4. The tests described in chapter 3 will help to verify this theoretical approach.

CHAPTER 3

EXPERIMENTAL WORK AND RESULTS

The tests conducted to verify the predictions of the suggested yield criterion were done in three major sections. These may be listed as:

a) Investigation of the stress-strain characteristics of the material used in various in-plane directions. This information is necessary to determine which set of perpendicular directions provide similar stress-strain characteristics to simulate initially isotropic material.

b) Stretching the sheet material in the x-direction to a total strain ε_x, followed by unloading which results in plastic strain ε_x^p. Subsequent stretching it in the y-direction provides useful information on the extent to which plastic straining alters the yield stress.

c) Bending the sheet material about the x-axis to a known radius and after allowing it to springback, stretching it in the x-direction.

Two types of aluminium alloys, Alcon 2S-H14 and 65S-O, were used throughout these experiments. Two types of alloys were used to study the influence of different degrees of strain hardening of the materials on the prediction of the theory. Alloy 2S-H14 had less strain hardening as compared to

alloy 65S-O. In each case sheets of three different thicknesses (1/8", 1/16" and 1/32") were used. Again, three material thicknesses were used to study the limitations of the theory when applied to a particular material.

The stress-strain characteristics for each sheet of both the materials were determined by ASTM standard tension tests. The tension test specimens were taken out in four directions, namely, parallel, perpendicular and at 45° and 135° to the direction of rolling. It was observed that the stress-strain curves for the first two directions varied considerably. However for the latter two directions the stress-strain curves were practically identical for all sheets except for 1/32 inch thick sheet of alloy 65S-O. As the theory assumes that the material is initially isotropic, it was desirable to have the stress-strain characteristics in two perpendicular directions the same. Hence all the specimens for the tests were taken out at 45° to the direction of rolling.

3.1 Stretching of Sheet:

As described earlier, this test consists of stretching the material in the x-direction and then unloading followed by stretching in the y-direction. Thus, to enable a coupon of sufficient length to be stretched in the y-direction after loading and unloading in the x-direction, a special

PHOTOGRAPH 3.1 MAIN SPECIMEN FOR SHEET-STRETCHING TEST

type of specimen, as shown in photograph 3.1, was used. The width of the specimen was kept 4 inches at centre and 2 inches at the ends. The width was reduced at the ends so as to allow the specimen to fit in the jaws of the testing machine. To avoid yielding of the material at the ends the thickness of the specimen was increased at these points. This was done by gluing one piece of material, cut to shape, on each face. Thus, the thickness of the specimen at the ends was three times that at the centre. Loctite adhesive 307 was used for this purpose to facilitate large strains to be introduced. The total length of the specimen was 2 feet so as to get a zone of uniform stress distribution in the central part of the specimen.

On each of these specimens, three strain gauges were mounted along the longitudinal centre-line, one at the centre and the other two at a centre to centre distance of 4 inches on either side of the first. It was observed that in almost all cases the strains were different, as indicated by strain gauges, at the three sections. However, the stress distribution across each section could be taken uniform. This was checked by mounting, on one of the specimens, two strain gauges, 1 inch centre to centre, on each of the three sections. The strains indicated by the two adjacent gauges were practically equal at all the sections.

Budd foil high elongation strain gauges, type HE-181B, with 120 ohm resistance were used. The tests were carried out on a 'Tinius Olsen' screw type testing machine. The specimens were loaded in tension at a constant strain rate of 0.005 inch/minute. The strains at the three sections were measured using a strain indicator and a multiple switch and balance unit. After introducing desired strains, the specimen was fully unloaded and the permanent strains were then measured at the three sections.

Next, three transverse strips, 1/2 inch wide, were cut out from the specimen in such a way that the centres of these coincided with the centre of the strain gauges. Each of these strips were properly marked for identification purpose. These were, then, shaped to a tension test specimen as specified by ASTM on a Tensil Cutter employing a template accessory. Budd foil strain gauges, type HE141-B, were mounted on each of these specimens. Then each was subjected to a tension test and the new stress-strain curve was obtained, from which the new yield stress for tension in the y-dimension was obtained. Photograph 3.2 shows a few transverse specimens after testing. The experimental data for this test is given in table 3.1.

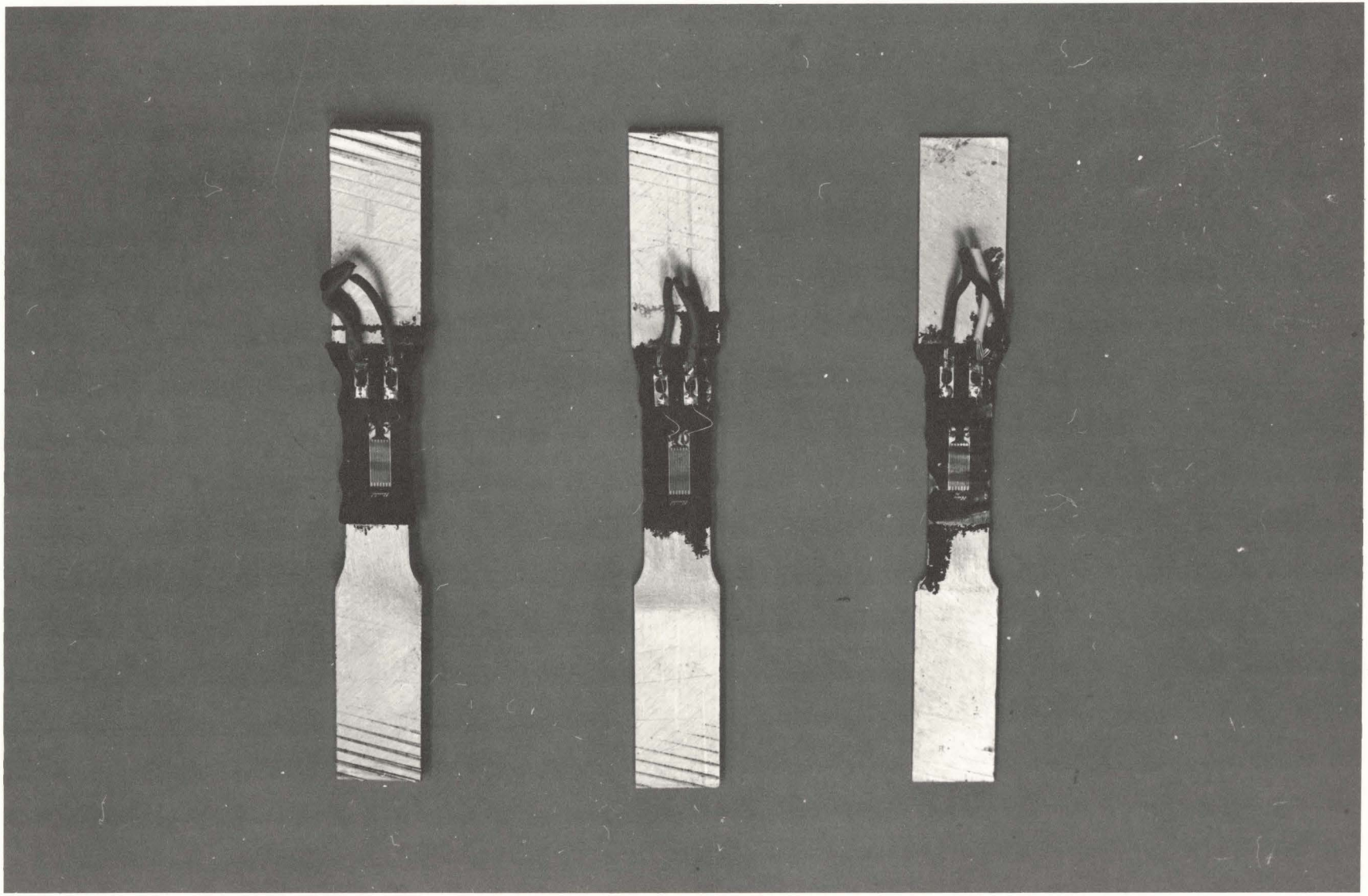

PHOTOGRAPH 3.2 TRANSVERSE SPECIMENS FOR SHEET-STRETCHING TEST

Sp.No.	Material	Thickness (inch)	Stress σ_x^t (psi)	Plastic strain ε_x^p (μ inch/inch)	σ_y^T(exp.) (psi)
A1-1	2S-H14	1/8	18485	8600	7900
A1-2	2S-H14	1/8	17800	2706	9050
A1-3	2S-H14	1/8	18440	7260	8150
A1-4	2S-H14	1/8	18480	8540	8000
A1-5	2S-H14	1/8	18010	3264	9050
A1-6	2S-H14	1/8	17970	3100	9080
A2-1	2S-H14	1/16	17000	3644	8250
A2-2	2S-H14	1/16	17400	11688	7400
A2-3	2S-H14	1/16	17100	4626	8000
A2-4	2S-H14	1/16	17280	5864	8800
A2-5	2S-H14	1/16	17300	8210	8500
A3-1	2S-H14	1/32	19093	4270	9150
A3-2	2S-H14	1/32	19420	11475	6400
A3-3	2S-H14	1/32	19210	6865	8200
A4-1	65S-0	1/8	10820	10280	6950
A4-2	65S-0	1/8	7850	2844	5150
A4-3	65S-0	1/8	8490	4020	5650
A4-4	65S-0	1/8	8830	4670	6050
A4-5	65S-0	1/8	9185	5610	6500
A4-6	65S-0	1/8	10700	9900	7700

Cont'd.

Sp.No.	Material	Thickness (inch)	Stress σ_x^t (psi)	Plastic strain ε_x^p (μ inch/inch)	σ_y^T (exp.) (psi)
A5-1	65S-0	1/16	12850	9780	4300
A5-2	65S-0	1/16	10510	3680	5200
A5-3	65S-0	1/16	12810	9542	4325
A5-4	65S-0	1/16	10875	4440	5150
A6-1	65S-0	1/32	14250	10470	8000
A6-2	65S-0	1/32	13125	4990	8900
A6-3	65S-0	1/32	14130	9495	8200
A6-4	65S-0	1/32	13100	4966	9150

Table 3.1 Test Data and Results For Sheet Stretching Test

3.2 Bending of Sheet:

For this test squire pieces, 9"×9", were cut out from the sheets at 45° to the direction of rolling for the reason explained earlier. These pieces were bent to a known radius employing a pyramid rolling press available in the machine shop. It consists of 3 No. 2-5/16 inch diameter rollers. One of these rollers can be screwed vertically alongside the other two rollers. These two rollers can be rotated manually by means of a gearing system, thus enabling the sheet to be rolled through the press to the radius of bend required. Sheeting was taken out of the press allowing it to springback elastically. In each case the radius of bend before and after elastic springback was measured.

Next, 3/4 inch wide strips were cut from the sheeting along the generators. These were shaped to ASTM standard tension specimens on the Tensil Cutter referred to earlier. Strain gauges, type HE181B, were mounted on each and the tension test was then carried out. The new stress-strain curve so obtained are compared with the predicted stress-strain curves in chapter 5. The radii, before and after springback, to which the various sheets were bent are given in table 3.2.

Specimen No.	Material	Thickness (inch)	Radius before Springback (inch)	Radius after Springback (inch)
B1-1	2S-H14	1/8	4.8	6.0
B1-2	2S-H14	1/8	7.2	10.0
B2-1	2S-H14	1/16	4.2	6.0
B2-2	2S-H14	1/16	2.5	3.0
B3-1	2S-H14	1/32	1.5	2.0
B3-2	2S-H14	1/32	2.0	3.0
B4-1	65S-0	1/8	13.0	14.0
B4-2	65S-0	1/8	15.8	18.0
B5-1	65S-0	1/16	4.5	6.0
B5-2	65S-0	1/16	3.0	4.0
B6-1	65S-0	1/32	2.5	3.0
B6-2	65S-0	1/32	3.0	4.0

Table 3.2 Test Data for Cold Bending Test.

CHAPTER 4

THEORETICAL PREDICTIONS

In this chapter theoretical predictions are made using the experimental data of chapter 3.

4.1 Sheet Stretching:

For each material, two arbitrary constants of the suggested yield criterion, m and n, can be calculated using the theoretical expressions (2.13) and two sets of experimental data. A typical calculation is shown below:

TYPICAL EXAMPLE:

Test Data:

Test No.	Thickness (inch)	Material	ε_x^p (inch/inch)	σ_x^t (psi)	σ_y^T(exp.) (psi)
Al-1	1/8	2S-H14	8600×10^{-6}	18485	7900
Al-2	1/8	2S-H14	2706×10^{-6}	17800	9050

Calculations:

Since, $$\sigma_y^T = \sigma_x^t - \frac{3m(1+2^n)}{2^{n+1}} (\varepsilon_x^p)^n \qquad (2.13)$$

For specimen Al-1,

$$7900 = 18485 - \frac{3m(1+2^n)}{2^{n+1}} (8600\times10^{-6})^n$$

or

$$\frac{3m(1+2^n)}{2^{n+1}} (8600\times10^{-6})^n = 10585 \qquad (a)$$

Similarly for specimen A1-2,

$$\frac{3m(1+2^n)}{2^{n+1}} (2706\times10^{-6})^n = 8750 \qquad \text{(b)}$$

Dividing (a) by (b),

$$(\frac{8600}{2706})^n = \frac{10585}{8750}$$

or,

$$n = 0.164.$$

Substituting the value of n in (b),

$$m = \frac{8750\times2^{1.164}}{3(1+2^{0.164})(2706\times10^{-6})^{0.164}}$$

or,

$$m = 8260.0 \text{ psi.}$$

The values of constants, m and n, depend on the stress-strain characteristics of the material. As the tensile stress-strain curves for the two materials, 2S-H14 and 65S-O, are different, different values of m and n for these should be expected. Since the stress-strain curve also varies with the thickness of the sheet, it was necessary to calculate the two constants separately for each sheet thickness of the material. The values of m and n thus calculated are tabulated in table 4.1. These values of m and n are used in expression (2.13) for predicting the new tensile yield stress in the y-direction for the remaining specimens. These are given in table 4.2.

Material	Thickness (inch)	m (psi)	n
2S-H14	1/8	8260	0.164
2S-H14	1/16	5740	0.114
2S-H14	1/32	15900	0.272
65S-0	1/8	7400	0.280
65S-0	1/16	31600	0.487
65S-0	1/32	27300	0.528

Table 4.1 Yield Criterion Constants

Sp. No.	Material	Thickness (inch)	Plastic strain ε_x^p (μ inch/inch)	σ_y^T (theoretical) (psi)
A1-1	2S-H14	1/8	8600	-
A1-2	2S-H14	1/8	2706	-
A1-3	2S-H14	1/8	7260	8140
A1-4	2S-H14	1/8	8540	7920
A1-5	2S-H14	1/8	3264	9000
A1-6	2S-H14	1/8	3100	9060
A2-1	2S-H14	1/16	3644	-
A2-2	2S-H14	1/16	11688	-
A2-3	2S-H14	1/16	4626	8100
A2-4	2S-H14	1/16	5864	8030
A2-5	2S-H14	1/16	8210	7780
A3-1	2S-H14	1/32	4270	-
A3-2	2S-H14	1/32	11475	-
A3-3	2S-H14	1/32	6865	8010
A4-1	65S-0	1/8	10280	-
A4-2	65S-0	1/8	2844	-
A4-3	65S-0	1/8	4020	5520
A4-4	65S-0	1/8	4670	5730
A4-5	65S-0	1/8	5610	5925
A4-6	65S-0	1/8	9900	6880

Cont'd.

Sp.No.	Material	Thickness (inch)	Plastic strain ε_x^p (μ inch/inch)	σ_y^T (theoretical) (psi)
A5-1	65S-0	1/16	9780	-
A5-2	65S-0	1/16	3680	-
A5-3	65S-0	1/16	9542	4410
A5-4	65S-0	1/16	4440	5065
A6-1	65S-0	1/32	10470	-
A6-2	65S-0	1/32	4990	-
A6-3	65S-0	1/32	9495	8220
A6-4	65S-0	1/32	4966	8900

Table 4.2 Theoretical Predictions for Sheet Stretching Test.

4.2 Sheet Bending:

The analysis outlined in this section shows a method to predict the gross stress-strain curve for tension in the x-direction after the sheet is bent, about the x-axis, to a known radius.

As described in chapter 2, the sheet thickness is divided into nine elements. The stress and strain are assumed to be constant throughout the element thickness. The bending process causes each of these elements to undergo different strains. When the bending force is removed elastic springback takes place and residual stresses are introduced if the initial bending involved plastic strains. The residual stress distribution, both in s and x directions, can be calculated by the method described in chapter 2. Since each element undergoes different strains during bending each will have a different yield surface associated with subsequent behaviour. The new yield stress for tension and compression in circumferential and longitudinal directions can be calculated for each element using the expressions (2.22 to 2. The value of the two constants m and n used are the same as obtained earlier in sec. 4.1. The new yield stresses are computed, for each case, using a computer. The program used is given in appendix 2. Now, a new yield surface for each fibre can be drawn.

Figure 4.1 shows the new yield surfaces and the residual stress distribution for test specimen B6-1, which has a thickness of 1/32 inch and is of aluminium alloy 65S-O. The points A,B,C,D and E, shown in this figure, represent the residual stress distribution of elements 1,2,3,4 and 5 respectively. For simplicity, only five yield surfaces corresponding to the five elements above and including the neutral axis are drawn. For defining the ellipses associated with the new yield surfaces the values of σ_s^T, σ_s^C, σ_x^T and σ_x^C, calculated earlier, are employed. The subsequent loading paths for tension in the x-direction can now be defined for each of five elements. For elements 6,7,8 and 9 only the loading paths DD", CC", BB" and AA" are shown to avoid confusion. For the elements, 1,2,3,4 and 5 loading in the x-direction after springback, is elastic for paths AA', BB', CC', DD' and EE' respectively. Thus AA', BB', CC', DD' and EE' represent the new effective yield stress ($\sigma_x^{T_e}$) for elements 1,2,3,4 and 5 respectively. Similarly DD", CC", BB" and AA" are the measures of new effective yield stress for elements 6,7,8 and 9 respectively.

When the specimen is loaded in tension in the x direction, each fibre remains elastic till it reaches its new effective yield stress. As AA' is the smallest ordinate, fibre 1 will be the first to yield if we impose the requirement that strains are equal for all elements in the x

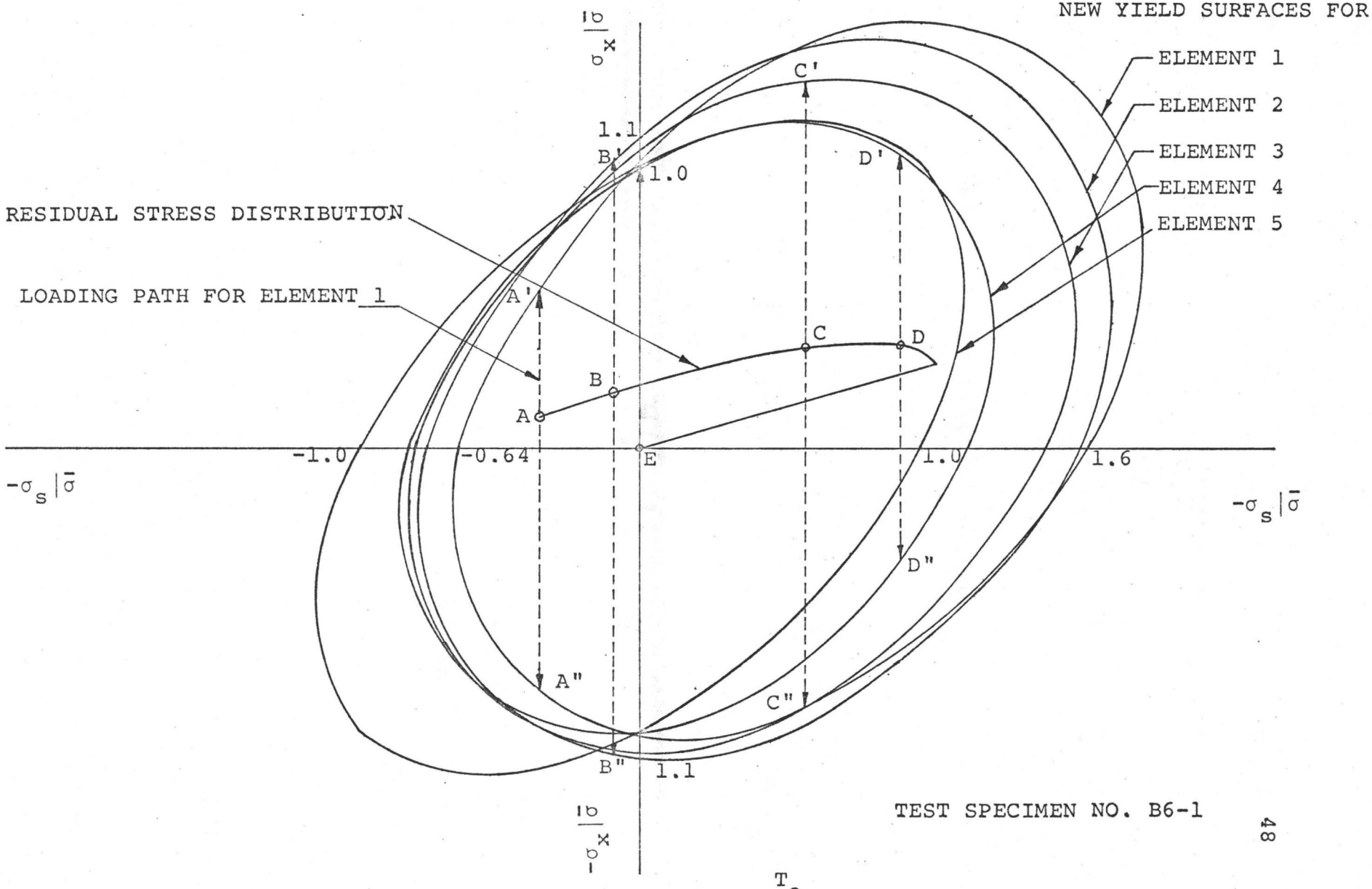

FIG. 4.1 NEW EFFECTIVE YIELD STRESSES ($\sigma_x^{T_e}$) FOR VARIOUS ELEMENTS

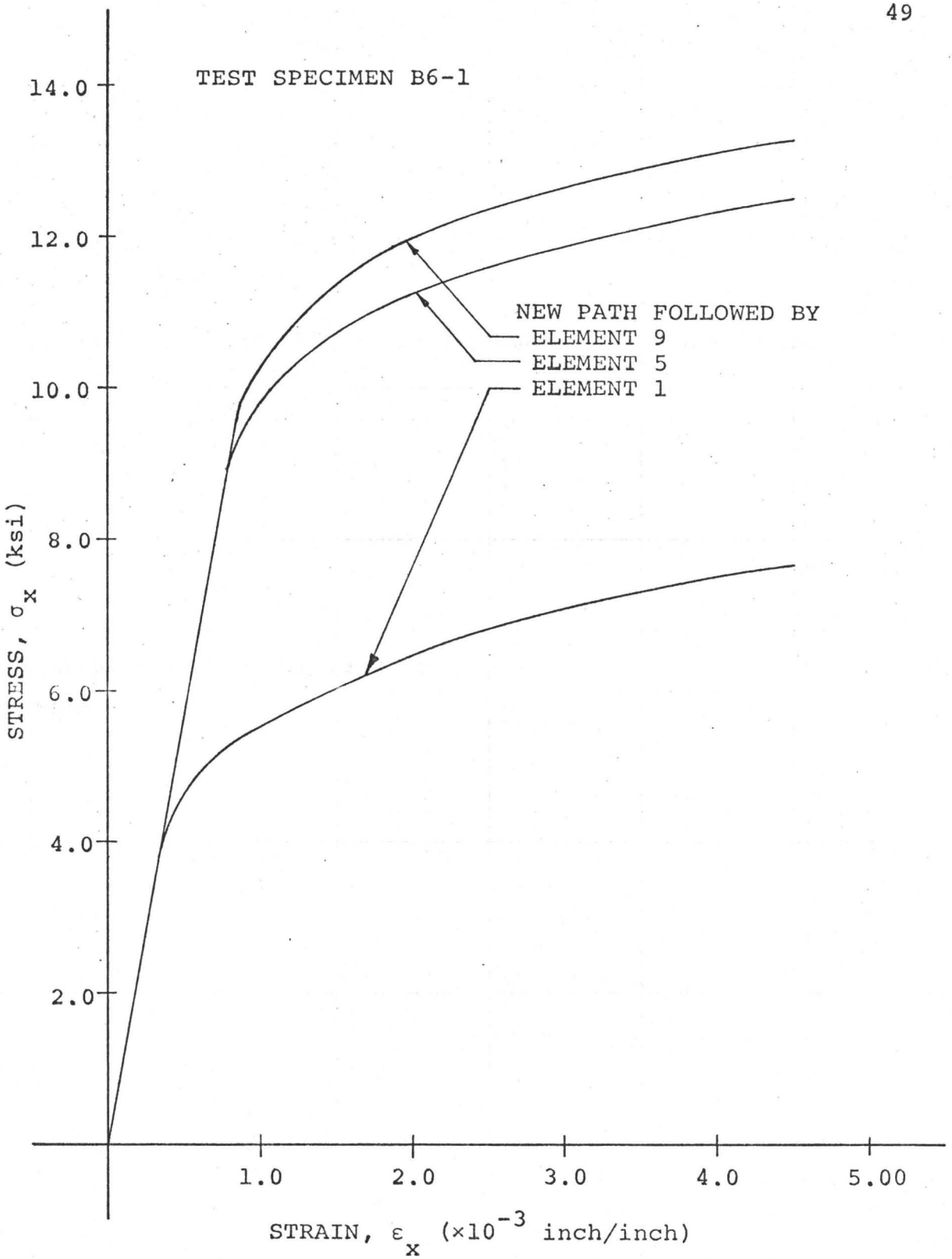

FIG. 4.2 TENSILE STRESS STRAIN RELATIONS FOR TYPICAL LONGITUDINAL ELEMENTS

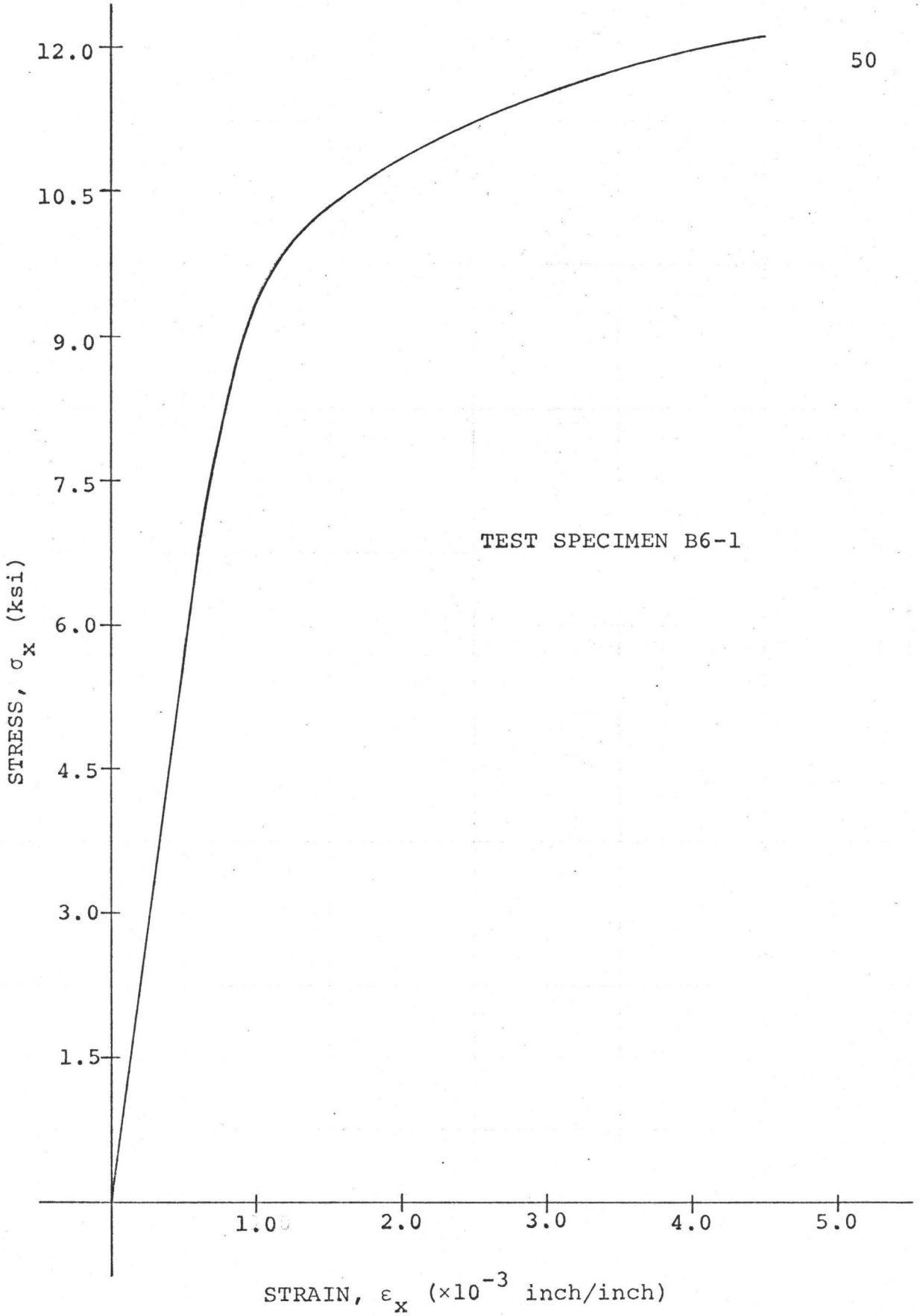

FIG. 4.3 THEORETICAL NEW TENSILE STRESS-STRAIN CURVE

direction. When the specimen is loaded beyond this point, all fibres except fibre 1 continue to be elastic until the next fibre reaches its new yield stress. For simplicity, it is assumed that the stress-strain characteristics beyond the new yield stress remain the same as that for a fibre without any strain history. Figure 4.2 shows the stress-strain curves for the outermost, central and the innermost fibres of the specimen. Using these types of curves, stress in each fibre can be calculated for any strain. Assuming the stresses to be constant over the thickness of the fibre an average stress can be calculated. The new stress-strain curve for tension in the x-direction is obtained by plotting ε_x vs. $\sigma_{x(\text{average})}$ as shown in fig. 4.3. The new stress-strain curves for all the specimens are given in chapter 5, where these are compared with the corresponding experimental curves.

CHAPTER 5

COMPARISON OF EXPERIMENTAL RESULTS WITH THEORY

5.1 Sheet Stretching Test:

The theoretical values of the revised yield stress, σ_y^T, as calculated in chapter 4 may be compared with the experimental values as shown in table 5.1. The comparison shows that in most of the cases two values are in good agreement. The maximum error in the results is about 10 percent which applies to test specimen A4.6. For all the cases where an error greater than 5 percent occurs it may be observed that the experimental values are greater. Thus, the theoretical predictions tend to be on the safe side.

5.2 Sheet Bending Test:

As described earlier, for this test, the experimental stress-strain curve for tension in the x-direction after bending is compared with the predicted gross stress-strain curve as calculated in chapter 4. A total of twelve specimens, two from each sheet of the two alloys, were subjected to bending. The subsequent gross stress-strain relations both theoretical and experimental are shown

Sp.No.	Material	Thickness (inch)	σ_y^T (exp.) (psi)	σ_y^T (theo.) (psi)	Error (%)
A1-1	2S-H14	1/8	7900	-	-
A1-2	2S-H14	1/8	9050	-	-
A1-3	2S-H14	1/8	8150	8140	0.12
A1-4	2S-H14	1/8	8000	7920	1.00
A1-5	2S-H14	1/8	9050	9000	0.00
A1-6	2S-H14	1/8	9080	9060	0.22
A2-1	2S-H14	1/16	8250	-	-
A2-2	2S-H14	1/16	7400	-	-
A2-3	2S-H14	1/16	8000	8100	-1.25
A2-4	2S-H14	1/16	8800	8030	8.75
A2-5	2S-H14	1/16	8500	7780	9.05
A3-1	2S-H14	1/32	9150	-	-
A3-2	2S-H14	1/32	6400	-	-
A3-3	2S-H14	1/32	8200	8010	2.37
A4-1	65S-0	1/8	6950	-	-
A4-2	65S-0	1/8	5150	-	-
A4-3	65S-0	1/8	5650	5520	2.30
A4-4	65S-0	1/8	6050	5730	5.30
A4-5	65S-0	1/8	6500	5925	8.80
A4-6	65S-0	1/8	7700	6880	10.60

Cont'd

Sp.No.	Material	Thickness (inch)	σ_y^T (exp.) (psi)	σ_y^T (theo.) (psi)	Error (%)
A5-1	65S-0	1/16	4300	-	-
A5-2	65S-0	1/16	5200	-	-
A5-3	65S-0	1/16	4325	4410	-1.97
A5-4	65S-0	1/16	5150	5065	1.62
A6-1	65S-0	1/32	8000	-	-
A6-2	65S-0	1/32	8900	-	-
A6-3	65S-0	1/32	8200	8220	-0.30
A6-4	65S-0	1/32	9150	8900	2.70

Table 5.1 Comparison of Results of Sheet Stretching Test

graphically in figures 5.1 to 5.12.

It may be observed that for alloy 2S-H14, which has a small degree of strain hardening there is remarkable accuracy in the results (figs. 5.1 to 5.6). In the small strain range, the two curves are almost identical. However, for higher strains the difference between the two curves is greater but within experimental accuracy. For alloy 65S-0, which has large strain hardening the deviation of the theoretical curve from its experimental counterpart is greater. This discrepancy in the results is to be expected in view of the approximations made in evaluating the stress-strain curves in bending. The method described in chapter 2 is an approximate method based on the equations derived for an elastic-plastic material by Alexander [13]. Strain hardening was taken into account by increasing $\bar{\sigma}$ in every cycle of computation. It was assumed that $\bar{\sigma}$ remained constant over a small increment of strain in each cycle. This is a good approximation for a material like alloy 2S-H14 which has a small degree of strain hardening. However for alloy 65S-O, having large strain hardening, a greater deviation is to be expected for the same strain increment with such an approximation.

A part of the discrepancy in the results can be accounted for by the fact that the experimental stress-

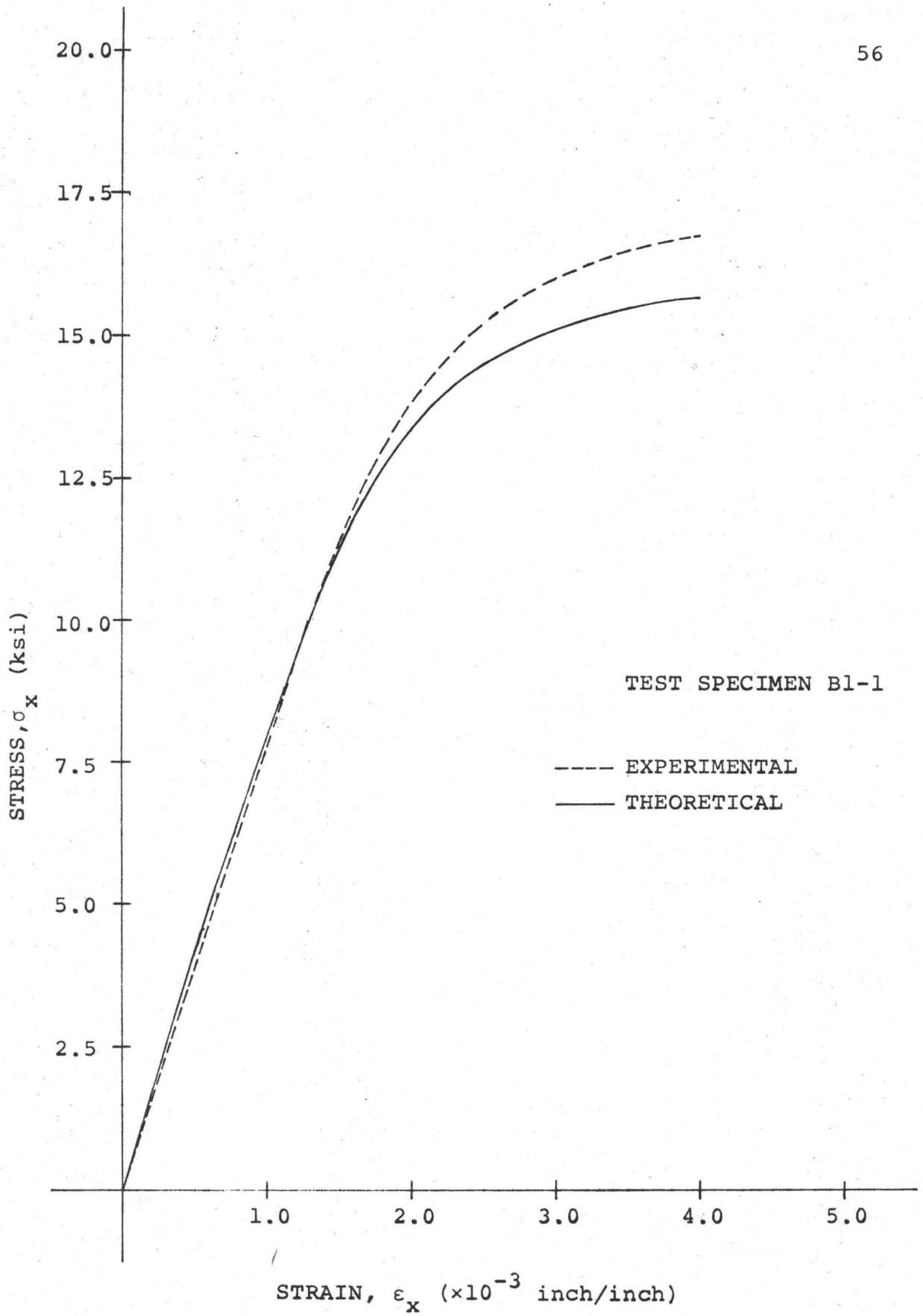

FIG. 5.1 NEW TENSILE STRESS-STRAIN CURVE

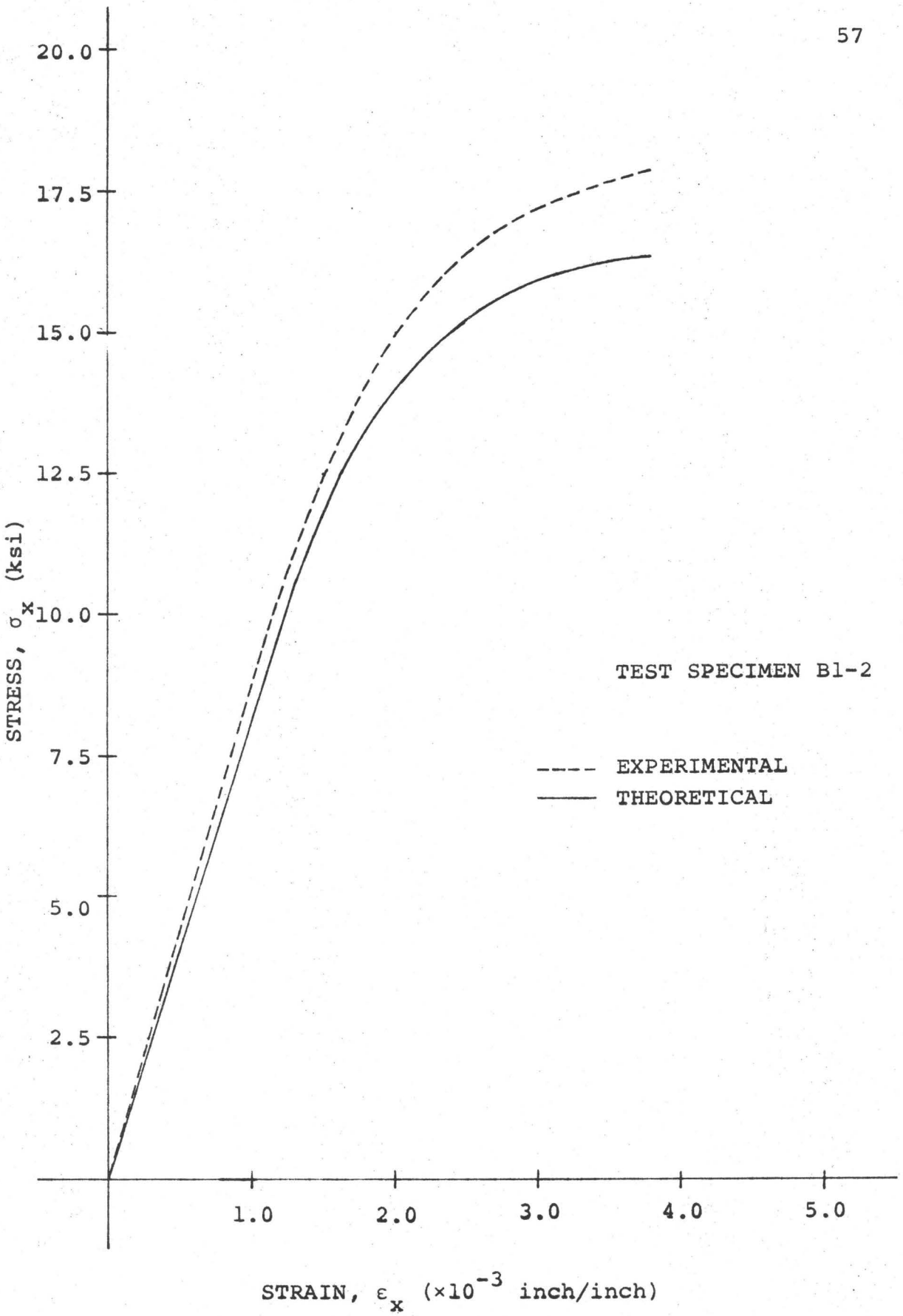

FIG. 5.2 NEW TENSILE STRESS-STRAIN CURVE

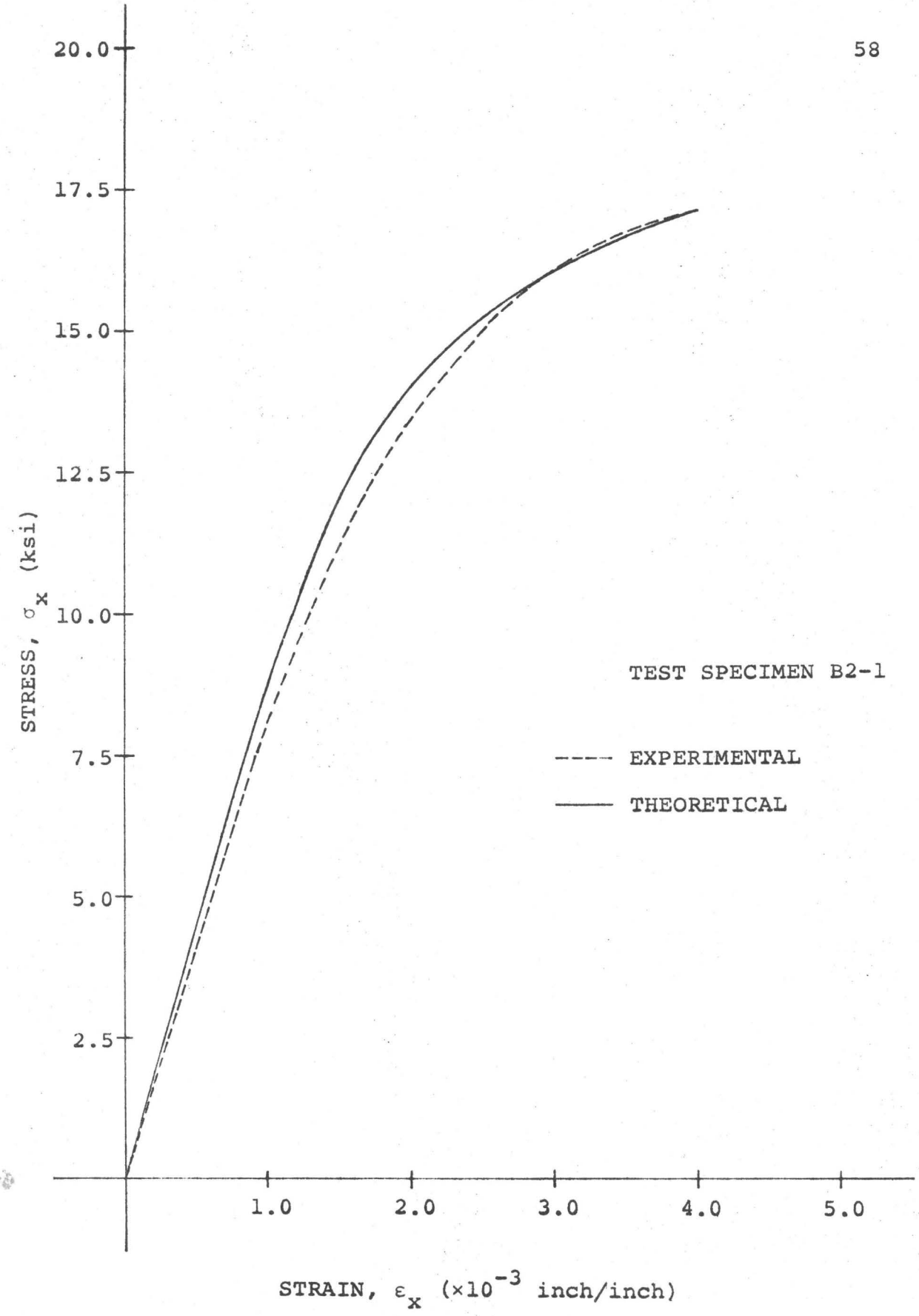

FIG. 5. 3 NEW TENSILE STRESS-STRAIN CURVE

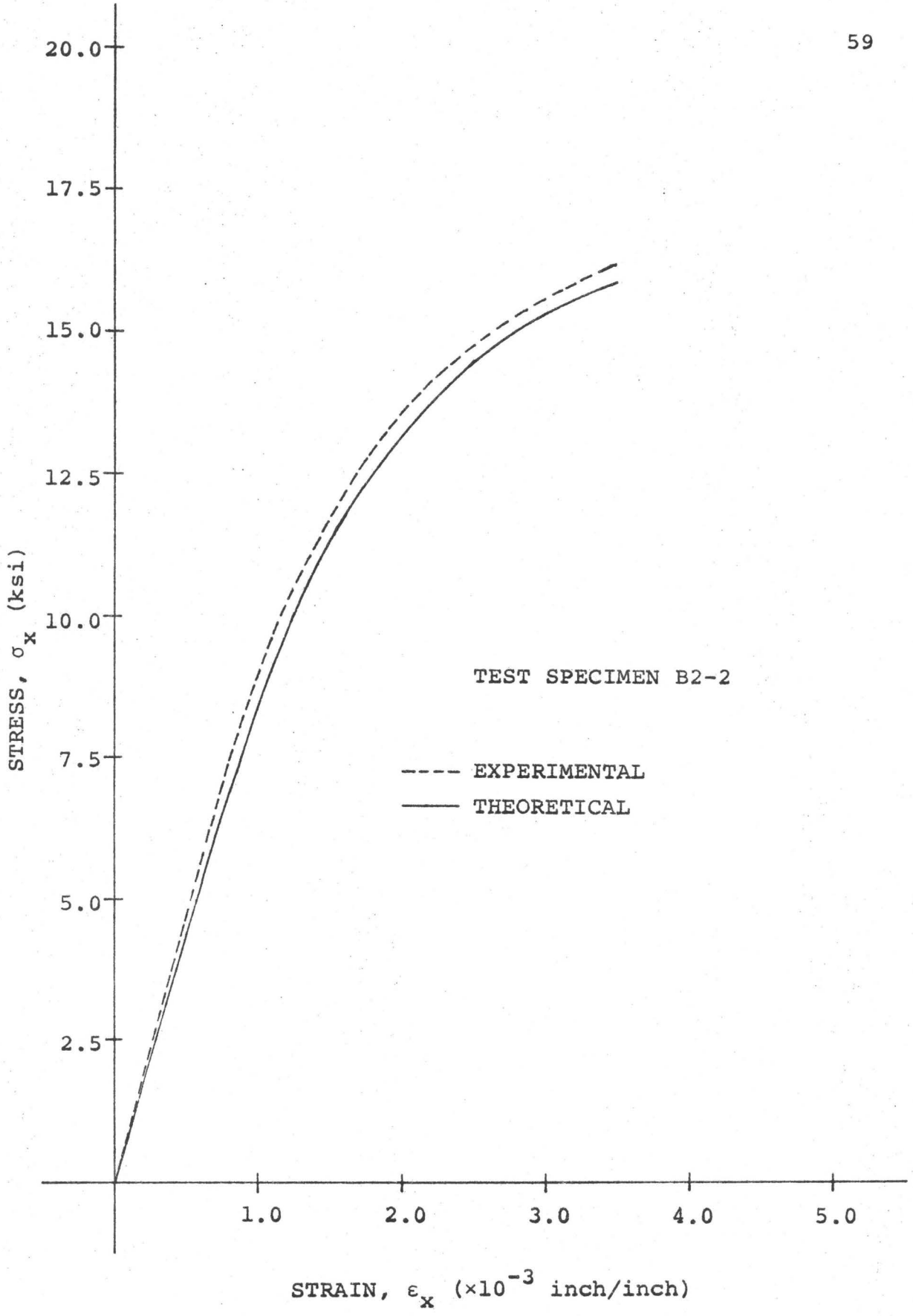

FIG. 5.4 NEW TENSILE STRESS-STRAIN CURVE

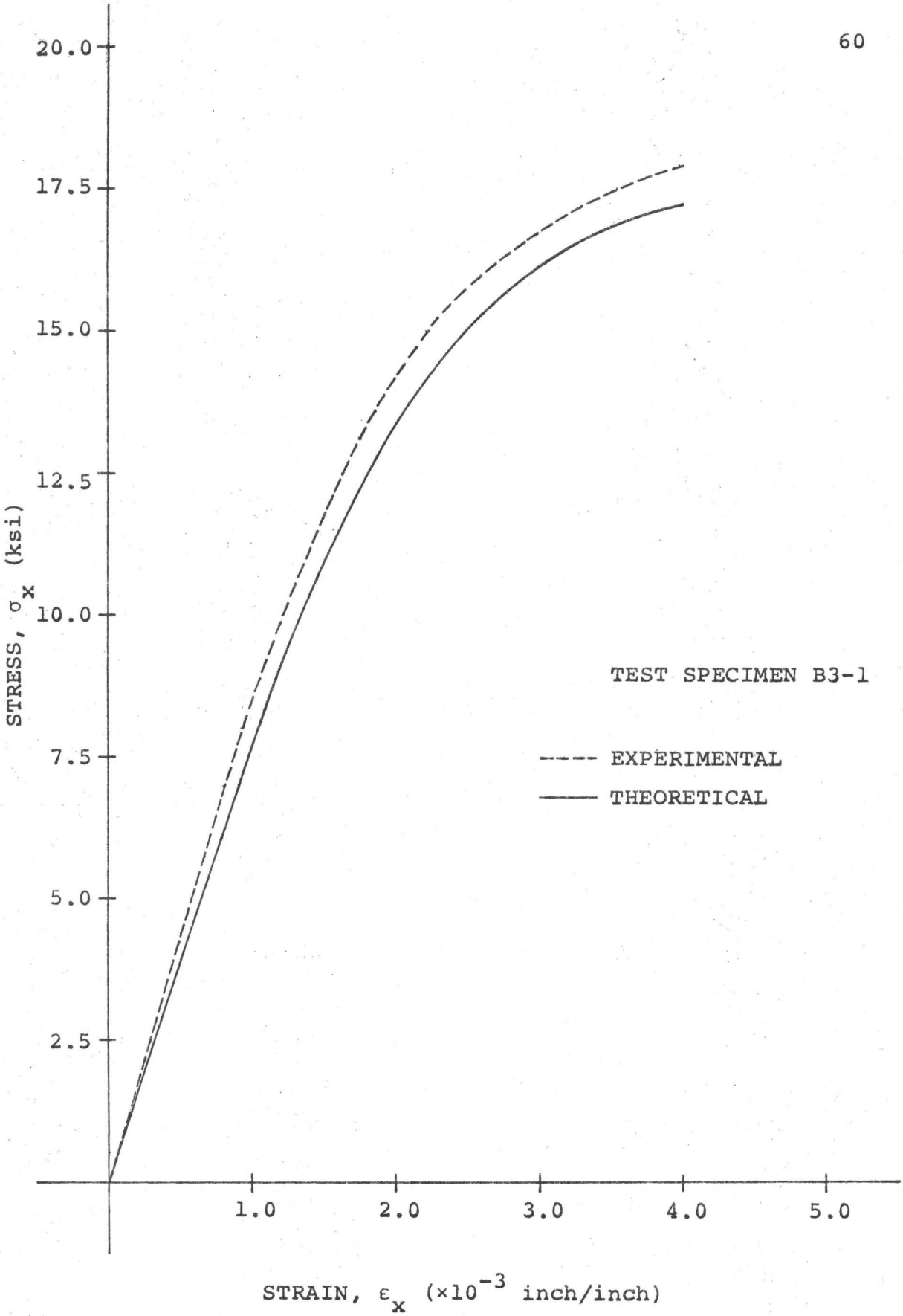

FIG. 5.5 NEW TENSILE STRESS-STRAIN CURVE

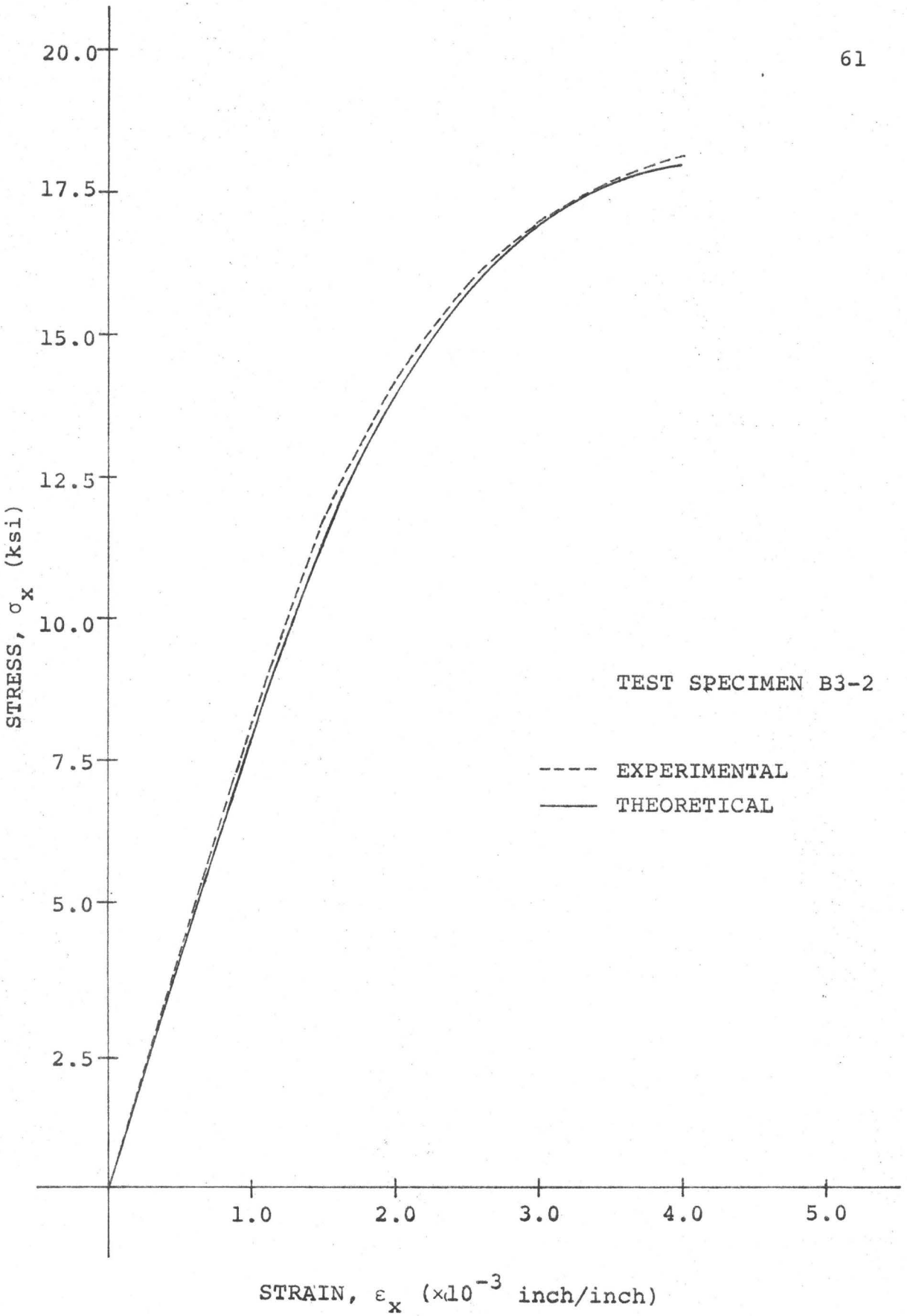

FIG. 5.6 NEW TENSILE STRESS-STRAIN CURVE

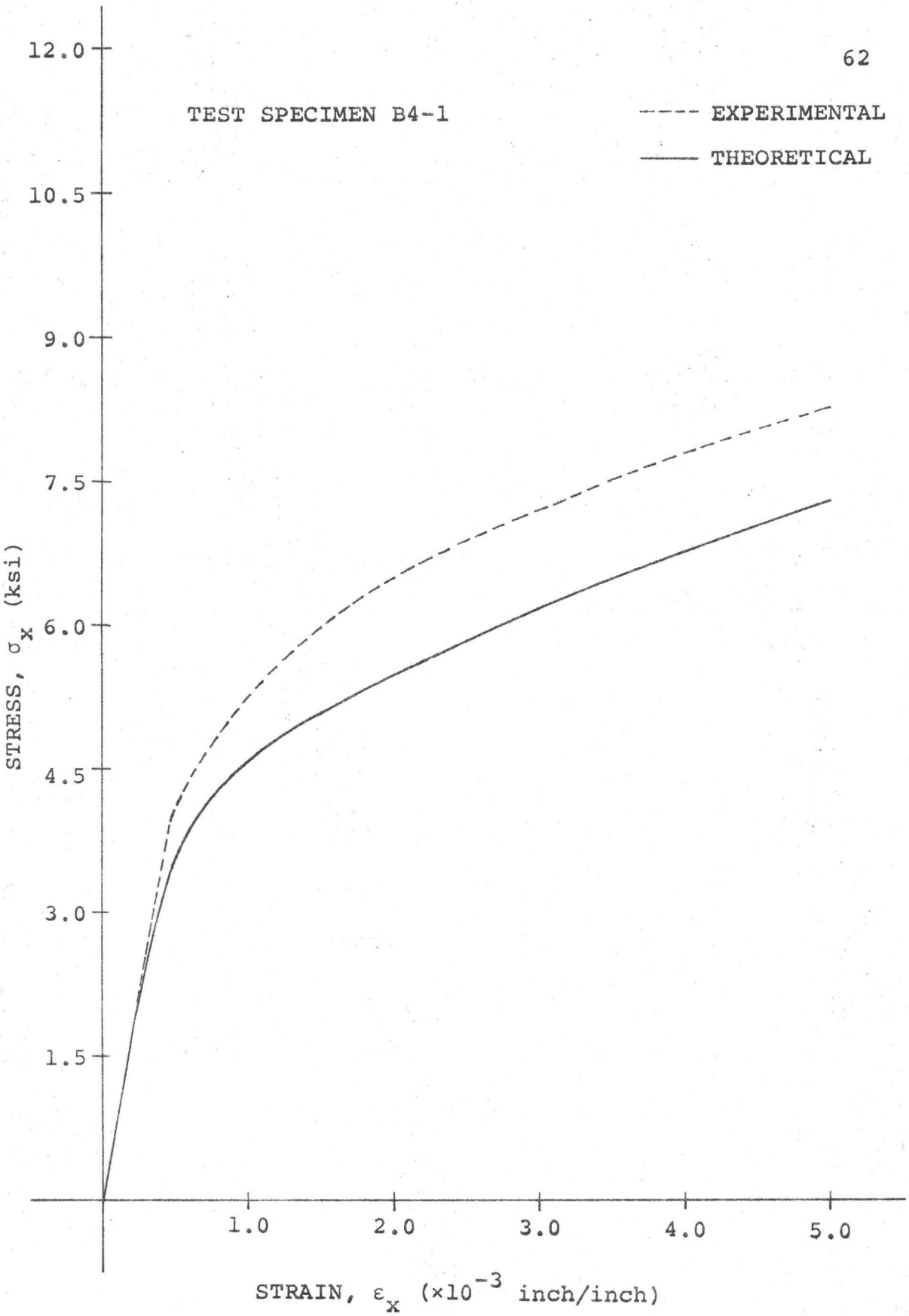

FIG. 5.7 NEW TENSILE STRESS-STRAIN CURVE

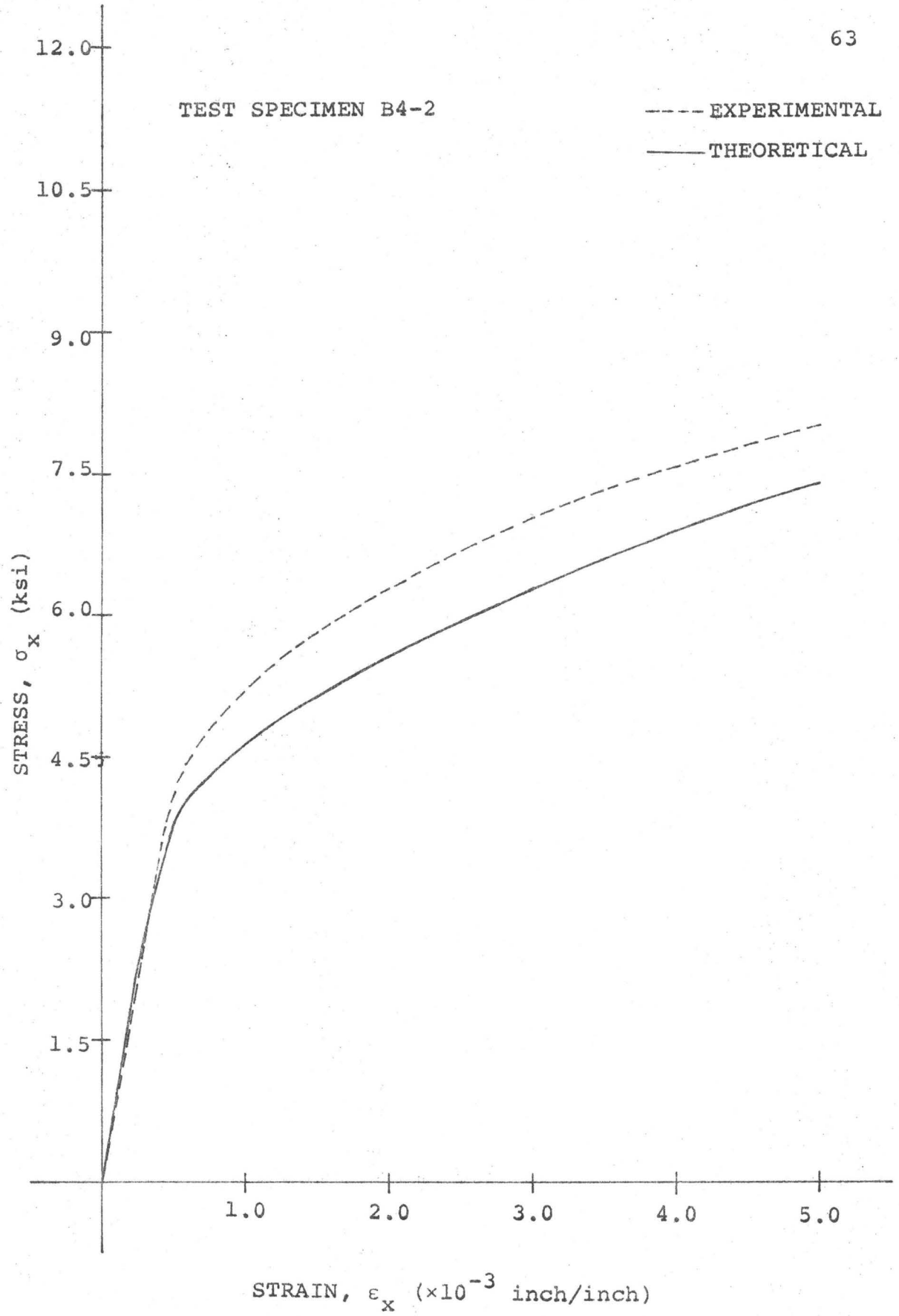

FIG. 5.8 NEW TENSILE STRESS-STRAIN CURVE

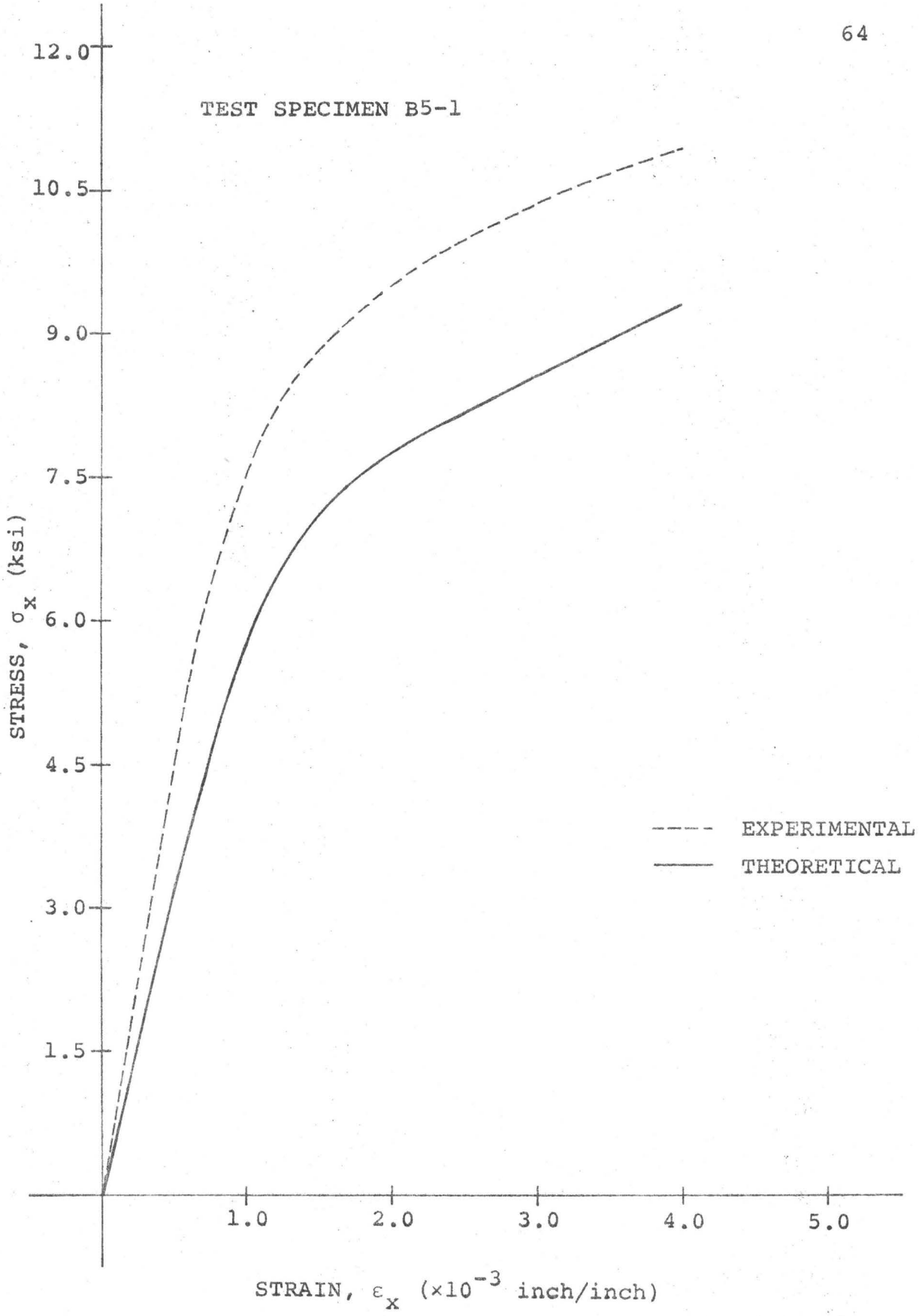

FIG. 5.9 NEW TENSILE STRESS-STRAIN CURVE

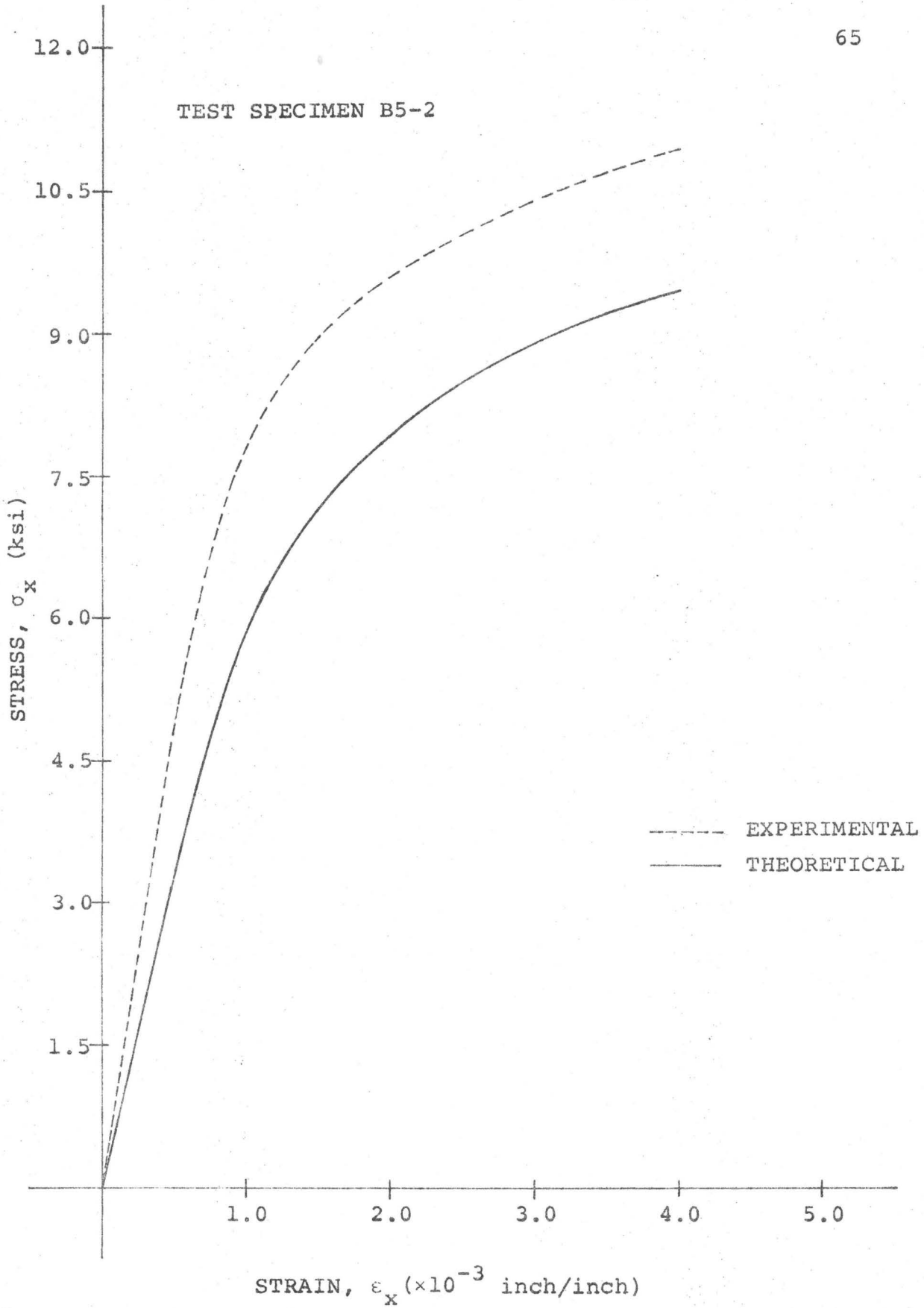

FIG. 5.10 NEW TENSILE STRESS-STRAIN CURVE

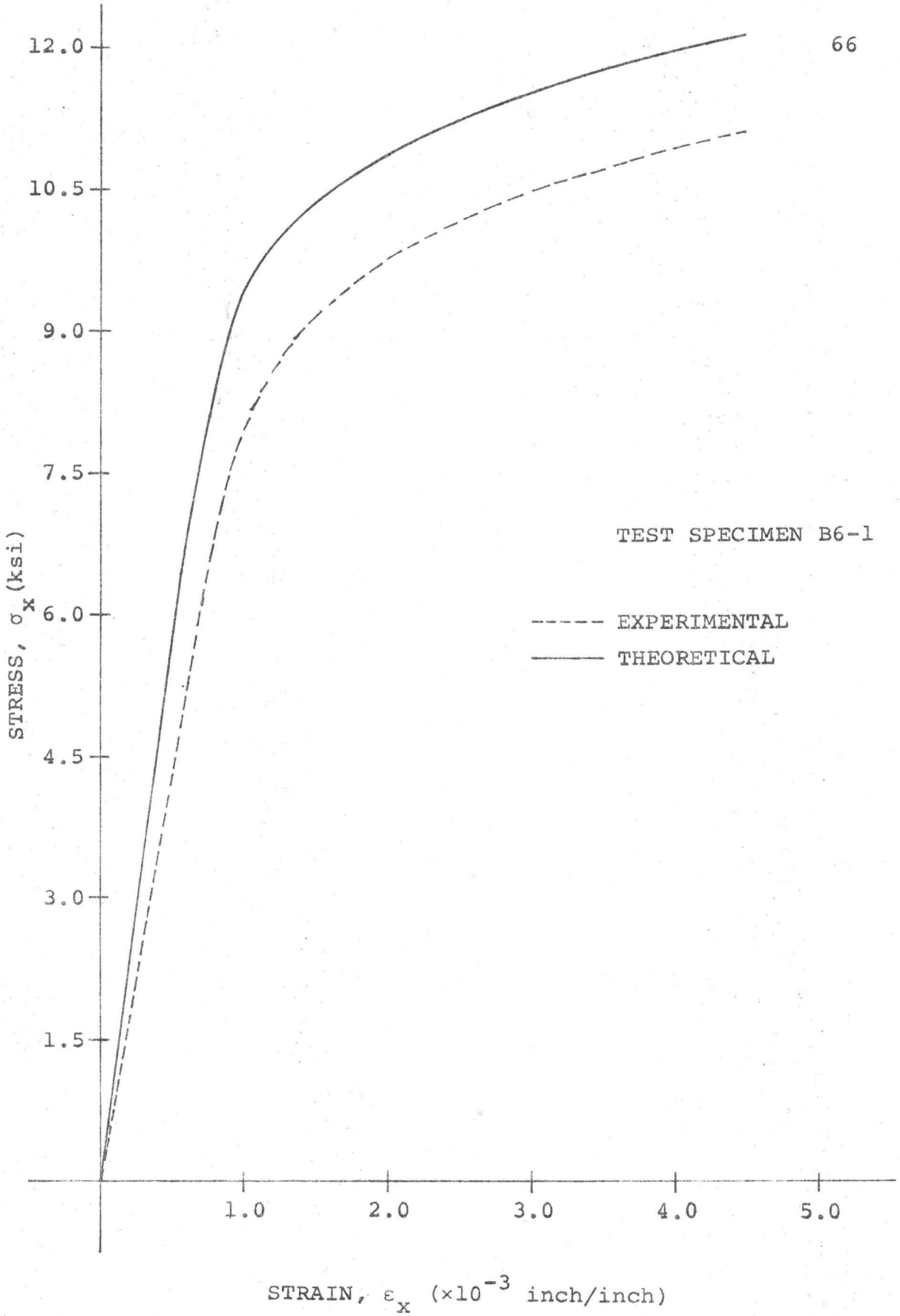

FIG. 5.11 NEW TENSILE STRESS-STRAIN CURVE

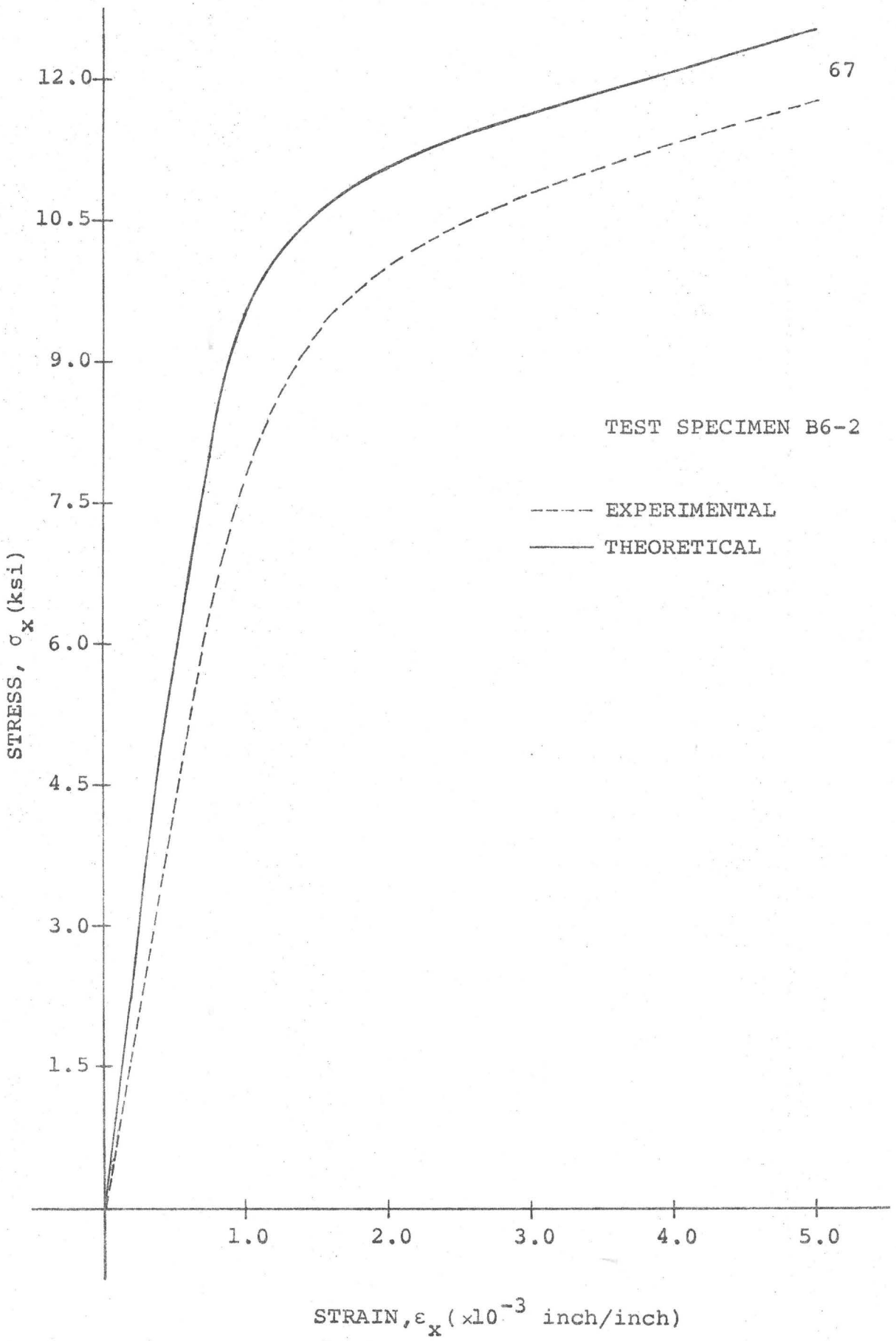

FIG. 5.12 NEW TENSILE STRESS-STRAIN CURVE

strain curves are not strictly for axial tension. As the specimens were cut from bent sheets, the cross-section of the specimen was curved. This results in a certain amount of eccentricity in loading. Thus, when the specimen is subjected to tension, strains as indicated by the strain gauge fixed on the concave side are due to an axial load and a bending moment. This error in the experiments could have been eliminated to a certain extent by fixing two strain gauges, one on either side of the specimen, and taking strain as the average of two readings. It is felt, however, that the eccentricity decreases with increasing load which tends to reduce the effect of bending moment. Test specimens B5-1, B5-2, B6-1 and B6-2 seem to have been affected most by the eccentricity.

Besides this, a few other factors could also have affected the experimental curve. The curved shape of the specimen not only introduces eccentricity in loading, it also tends to straighten the specimen during tensile loading. This will affect the residual stress distribution and the curvature of the specimen about the x-axis. It is difficult to calculate the error involved due to this type of loading. However, considering the length of the specimen it is felt that the straightening effect will be small at the centre of the specimen.

For both stretching and bending test a number of specimens of each alloy were tested with different loading

histories so as to check the accuracy of the theory. It is desirable to check the reliability of the experimental results by testing a number of specimens having the same loading history. Due to limitation of time this approach was not feasible, however. The reliability of the experimental work can, however, be justified to a certain extent by the fact that the variation of σ_y^T due to the plastic strain ε_x^p appears to be continuous.

It may be observed that except for test specimens B6-1 and B6-2, cut from 1/32 inch thick sheet of alloy 65S-0, the experimental curve is always above the predicted curve. This suggests that the predictions made are on the safe side. The discrepancy in test specimens B6-1 and B6-2 may be due to the assumption made that the material is isotropic initially. The uniaxial stress-strain curves for the chosen perpendicular directions were the same for all sheets except for the 1/32 inch thick sheet of 65S-0 alloy. For this particular sheet there was an appreciable difference in the two stress-strain curves.

Considering all of these approximations it can be concluded that the predictions made using the suggested yield criterion are reasonably safe and accurate.

CHAPTER 6

CONCLUSIONS

The proposed yield criterion which is a modification to the common Von Mises type takes into account the effect of plastic strain history on subsequent behaviour. The loading function as applied herein is simple to use and gives answers which are on the safe side in contradistinction to most strain hardening theories as employed with metals.

As applied to an aluminium alloy Alcon 2S-H14 exhibiting a relatively small degree of strain hardening

a) the yield point in uniaxial tension in a direction perpendicular to that for original tensile loading is predictable to within about 10.0 percent for $\varepsilon_x^p \doteq 12000$ micro inches/inch.

b) the yield point in uniaxial tension following a cold bending process in a perpendicular direction is predicted to be much lower than would be the case without sheet bending for radius to thickness ratios in the range 40 to 70.

c) the stress-strain curves are predicted from theory for the loading histories of a) and b) within 6% for strains of 0.4%.

As applied to an aluminium alloy Alcon 65S-0 which

exhibits considerable strain hardening

a) the yield point in uniaxial tension in a direction perpendicular to that for original tensile loading, is predictable to within about 11 percent for $\varepsilon_x^p \doteq 10000$ micro inches/inch.

b) the yield point in uniaxial tension following a cold bending process in a perpendicular direction is predicted to be much lower than would be the case without sheet bending for radius to thickness ratios in the range 95 to 125.

c) the stress-strain curves are predicted from theory for loading histories of a) and b) within 15% for strains of 0.4%.

The yield criterion should not be used for strongly anisotropic materials as illustrated by some of the tests. Predictions for the mildly anisotropic sheets as employed herein deviated as much as 8% for strains of 0.4%. These results were also found to be on the unsafe side.

Suggestions for Future Research

1. In this work, the subsequent behaviour of an isotropic material after plastic straining has been checked only for tensile loading. This really does not prove its complete validity. This theory needs a check by loading in compression in the two principal directions. A more complex loading system than simple tension would help to ascertain the validity of an essentially Von Mises criterion.

2. Test for initially anisotropic materials: Evaluate the six parameters F,G,H,L,M and N which connect the increments of stress and plastic strains as described by Hill [4]. Once the principal axes have been determined an application of the simplified theory described herein should be investigated to determine whether a reasonably simplified approach can be applied to a most complex problem.

APPENDIX 1

```
C TO CALCULATE STRESS-STRAIN CURVE FOR BENDING
C UNIAXIAL STRESS-STRAIN CURVE IS DIVIDED INTO SMALL PARTS DEFINED BY
C (STR1,SIG1)ETC.
C V=POISSONS RATIO IN ELASTIC RANGE
C POI=POISSONS RATIO IN PLASTIC RANGE IT VARIES WITH STRAIN
      WRITE(6,300)
 300  FORMAT(40X,8HMATERIAL,3X,6H2S-H14/)
      WRITE(6,130)
 130  FORMAT(2X,9HTHICKNESS,5X,1HY,5X,8HCONSTANT,11X,5HSIGMS,11X,5HSIGMX
     1,9X,6HSTRAIN,8X,3HPOI/)
      DO 99 I=1,6
      IF(I.NE.4)GO TO 25
      WRITE(6,66)
 66   FORMAT(40X,8HMATERIAL,4X,5H65S-O/)
 25   V=0.3
      POI=0.3
      READ(5,100)THICK,Y
  100 FORMAT(F10.5,F8.1)
      READ(5,101)STRI,STR1,STR2,STR3,STR4,STR5
 101  FORMAT(6F10.6)
      READ(5,102)SIG1,SIG2,SIG3,SIG4,SIG5
 102  FORMAT(5F10.1)
      READ(5,103)Z0,Z1,Z2,Z3,Z4,Z5
 103  FORMAT(6E12.4)
      E=Y/STRI
      YO=Y
      SIGMX=0.34
 89   C=Y*(SQRT(3.0)/4.0)*ALOG(ABS((2.0*SQRT(1.0-V+V**2)-SQRT(3.0))/(2.0
     1*SQRT(1.0-V+V**2)+SQRT(3.0))))-(1.0-2.0*V)*V*Y/SQRT(1.0-V+V**2)
      SIGMS=(SQRT(SIGMX**2-4.0*(SIGMX**2-1.0))+SIGMX)/2.0
      A=(1.0-2.0*V)*SIGMX*Y-((SQRT(3.0)*Y)/4.0)*ALOG(ABS((2.0-SQRT(3.0)*
     2SIGMS)/(2.0+SQRT(3.0)*SIGMS)))+C
      STRAIN=(A+Y*(1.0-V**2)/SQRT(1.0-V+V**2))/E
      X=SQRT(1.0-POI+POI**2)/(1.0-POI**2)
      ST=X*STRAIN
      IF(ST.LE.STR1)GO TO 44
      IF(ST.LE.STR2)GO TO 45
      IF(ST.LE.STR3)GO TO 46
      IF(ST.LE.STR4)GO TO 47
      IF(ST.LE.STR5)GO TO 48
      GO TO 49
 44   S=YO+Z0*(ST-STRI)
      GO TO 50
 45   S=SIG1+Z1*(ST-STR1)
      GO TO 50
 46   S=SIG2+Z2*(ST-STR2)
      GO TO 50
```

CONTD.

```
47    S=SIG3+Z3*(ST-STR3)
      GO TO 50
 48   S=SIG4+Z4*(ST-STR4)
      GO TO 50
 49   S=SIG5+Z5*(ST-STR5)
 50   SIGMX=SIGMX*Y/YO
      SIGMS=SIGMS*Y/YO
      STRAIN=STRAIN/STRI
      POI=SIGMX/SIGMS
      WRITE(6,30)THICK,Y,C,SIGMS,SIGMX,STRAIN,POI
 30   FORMAT(F10.5,2F10.1,6X,F10.3,6X,F10.3,6X,E12.6,F8.3)
      SIGMX=SIGMX*YO/Y
      Y=S
      IF(STRAIN.GE.15.0)GO TO 99
      IF(POI.GE.0.50)GO TO 99
      SIGMX=SIGMX+0.01
      GO TO 89
 99   CONTINUE
      STOP
      END
```

```
C TO CALCULATE NEW YIELD STRESSES IN TENSION AND COMPRESSION ALONG
C S AND X DIRECTIONS AFTER COLD BENDING OF SHEETS
C M=A,N=B AS THE CONSTANTS ARE NOT INTEGERS
C POI=AVERAGE POISSONS RATIO
      WRITE(6,23)
   23 FORMAT(40X,8HMATERIAL,3X,6H2S-H14//)
      WRITE(6,2)
    2 FORMAT(2X,9HTHICKNESS,2X,6HRADIUS,4X,3HZ/A,5X,6HSTRAIN,11X,5HSIGST
     1,10X,5HSIGSC,8X,5HSIGXT,9X,5HSIGXC,4X,3HPOI//)
      DO 3 I=1,60
      IF(I.NE.31)GO TO 24
      WRITE(6,22)
   22 FORMAT(40X,8HMATERIAL,3X,5H65S-O//)
   24 READ(5,4)THICK,RAD,RA,A,B,S,ST,SE,POIF
    4 FORMAT(F8.5,F6.2,F5.2,F8.1,F6.3,E11.5,F9.1,E12.5,F7.3)
      IF(SE.EQ.0.0)GO TO 20
      POI=(POIF-0.30)*S/SE+0.30
      GO TO 30
   20 POI=POIF
   30 X=SQRT((ST-1.5*A*S**B)**2-POI*(1.0-POI)*ST**2)
      Y=1.5*A*S**B
      Z=(1.0-POI+POI*POI)
      Q=SQRT(Z*ST**2-3.0*A*ST*S**B)
      SIGST=X+Y
      SIGSC=X-Y
      SIGXT=Q
      SIGXC=Q
  200 WRITE(6,10)THICK,RAD,RA,S,SIGST,SIGSC,SIGXT,SIGXC,POI
   10 FORMAT(F10.5,F8.1,F8.2,E14.5,4F14.1,F6.3/)
    3 CONTINUE
      STOP
      END
```

REFERENCES

1. Drucker, D.C. "The Significance of the Criterion for Additional Plastic Deformation of Metals" Rheology issue, Journal of Colloid Science Vol. 4, No. 3, pp 299-311, 1949.

2. Drucker, D.C. "Relation of Experiments of Mathematical Theories of Plasticity". Journal of Applied Mechanics Trans. ASME, Vol. 71, pp 349-357, 1949.

3. Reuss, A. "Anisotropy Caused by Strain". Proc. 4th International Congress of Applied Mechanics, Cambridge, England. p.241, 1934.

4. Hill, R. "Mathematical Theory of Plasticity". Oxford, 1950.

5. Edelman, F. and Drucker, D.C. "Some Extension of Elementary Plastic Theory" Journal of Franklin Institute, Vol. 251, pp. 581-605, 1951.

6. Naghdi, P.M., Essenburg, F., Koff, W. "An Experimental Study of Initial and Subsequent Yield Surfaces in Plasticity". ASME Vol. 79 , pp 201-209, 1957.

7. Chajes, A., Britvec, S.J. and Winter, G. "Effect of Cold Straining on Structural Sheet Steel". Proc. ASCE, Structural Div., Vol. 89, pp 1-32, April 1963.

8. Karren, W.K. "Corner Properties of Cold-Formed Steel Shapes". Proc. ASCE, Structural Div., Vol. 93, pp 401-432, February 1967.

9. Karren, W.K. and Winter, G. "Effect of Cold Forming on Light-Gage Steel Members". Proc. ASCE, Structural Div. Vol. 93, pp 433-470, February 1967.

10. Batterman, S.C. "Plastic Buckling of Axially Compressed Cylindrical Shells", AIAA Journal, Vol. 3, No. 2, pp 316-325, February 1965.

11. Prager, W. "The Theory of Plasticity: A Survey of Recent Achievements", Proc. Instn. Mech. Engrs. Vol. 169, pp 41-57, 1955.

12. Fung, Y.C., Wittrich, W.H. "A Boundary Layer Phenomenon in the Large Deflexion of Thin Plates", Quart. Journal Mech. and App. Math., Vol. VIII, Pt. 2, 1955.

13. Alexander, J.M. "An Analysis of the Plastic Bending of Wide Plate and the Effect of Stretching on Transverse Residual Stresses", Proc. Instn. Mech. Engrs., Vol. 173, No. 1, pp 73-85, 1959.

14. Daniels, L.R. "The Influence of Residual Stress Due to Cold Bending on Thin-Walled Open Sections", M. Eng. Thesis, McMaster University, 1969.